COMPUTATIONAL FLUID DYNAMICS OF AIR CIRCULATION IN A ROOM

A DISSERTATION

Submitted in partial fulfillment of the
requirements for the award of the degree
of
MASTER OF TECHNOLOGY
in
CHEMICAL ENGINEERING
(With Specialization in Industrial Safety and Hazards Management)

By

GIRADA RAMINAIDU

DEPARTMENT OF CHEMICAL ENGINEERING
INDIAN INSTITUTE OF TECHNOLOGY ROORKEE
ROORKEE-247 667 (INDIA)

JUNE, 2007

CANDIDATE'S DECLARATION

I hereby declare that the work, which is being presented in the dissertation, entitled, **"COMPUTATIONAL FLUID DYNAMICS OF AIR CIRCULATION IN A ROOM"** submitted in partial fulfillment of the requirements for the award of degree of **Master of Technology** in Chemical Engineering with specialization in **"INDUSTRIAL SAFETY AND HAZARDS MANAGEMENT"** submitted in the Department of **CHEMICAL ENGINEERING**, Indian Institute of Technology Roorkee, India, is an authentic record of my own work carried out under the supervision of **Dr. R. BHARGAVA.**

The matter embodied in this dissertation has been submitted by me for the award of any other degree.

Date: 28th june, 2007
Place: Roorkee

G. Raminaidu
(GIRADA RAMINAIDU)

CERTIFICATE

This is to certify that above statement made by candidate is correct to best of my knowledge and belief.

R Bhargava

Dr. R. Bhargava,
Assistant Professor,
Department of Chemical Engineering,
Indian Institute of Technology Roorkee,
INDIA—247667.

ACKNOWLEDGEMENTS

I am greatly indebted to my guide Dr. R. BHARGAVA, Assistant Professor, Department of Chemical Engineering, Indian Institute of Technology Roorkee for his kind support and guidance during the entire course of this work. His cooperation and indepth knowledge have made my work possible.

I am also thankful to Dr. SHRICHAND, Head of the Department, Chemical Engineering Department and other staff members for their instant help in all kinds of work.

I would like to thank Maharshi subhash, M.Tech 2^{nd} year for helping to work on FLEUENT.

I would like to thank my friends for their continuous support and enthusiastic help.

Last but not the least, it is all owed to the blessings of my parents, brother and God that I have come up with this work in due time.

(GIRADA RAMINAIDU)

ABSTRACT

In ventilated or air-conditioned rooms optimal conditions of temperature, humidity and air velocity are required. Literature has reported that computational fluid dynamics (CFD) methods have been used to investigate the velocity and temperature fields in a mechanically ventilated enclosure. Effort has been to investigate the indoor air quality of the system under study. The present work is numerical simulation of room air flow having multiple inlet and outlets using CFD code.

In this study the air flow in a small size room is simulated using CFD code FLUENT 6.2.16, to predict the behaviour of the air flow a numerical scheme was used to solve the conservation equations for mass, momentum and energy with the k-ϵ turbulence model.

In this work two models of a Room are considered. Room is having one inlet, two windows and four exhausts. The dimensions of room are: length is 6 m, width is 6 m and height is 4.5 m. The inlet is 2.5 m height and 1.5 m width and is located on the left wall of the room at z= 2.25 m. The windows are 2 m length and 1 m height, one is located on the front wall at a height of y=1 m and the other one is located on the back wall at the same height. Exhausts are of circular shape having 0.5 m radius. Two exhausts are on the right wall at height of 3 m at z=1 m and z= 5 m respectively. Other two exhausts are on the ceiling of the room at x=2 m, z=1.5 m and x= 2 m, z= 4.5 m respectively. In one model, wall temperature differentials are considered whereas in the other one wall temperatures are constant temperature.

For both cases the vector plots of velocity and contour plots of air velocity are studied. The inlet velocity is 1 m/s. The suction pressure of exhausts is 0.3 bar. For the wall temperature differential model the temperature profiles are studied.

CONTENTS

LIST OF FIGURES

LIST OF TABLES

NOMENCLATURE

A	Area	(m^2)
D	Mass divergence	(1/s)
G	Acceleration due to gravity	(m/ s^2)
H	Total height of opening	(m)
K	Thermal conductivity	(W/(m K))
k	Turbulent kinetic energy	(m^2/s^2)
P	Pressure	(Pa)
Q	Volumetric flow rate	(m^3/s)
t	Time	(s)
T	Temperature	(K)
U, V, W	Velocity components in x, y, and z-directions	(m/s)
Ain, Aout	Inlet and outlet cross-sectional areas	(m^2)
C_d	Discharge coefficient	
$C\mu$, C_1, C_2	Constants for the k-ε model	
Cp	Specific heat	(J/(kg K))
$F\mu$, F1, F2, E	Empirical functions for the k-ε model	
g_i, g_j, g_k	Tensor notation for gravitational acceleration	(m/s^2)
k_{in}	Turbulent energy at room inlet	(m^2/s^2)
q"	Heat flux vector	(W/m^2)
y_n	Normal distance	(m)
x_i, x_j, x_k	Tensor notation for principle directions	
x_n	Normal direction	
R_T	Turbulent Reynolds number	
R_y	Local Reynolds number	
To	Reference temperature	(K)
U_0	Inlet velocity	(m/s)
U_t	Tangential velocity	(m/s)
Un	Normal Velocity	(m/s)
Uout	Outlet velocity	(m/s)
U_i, U_j, U_k	Tensor notation for velocity components	(m/s)
$U_{i,j,k}$	U velocity at cell (i,j,k)	(m/s)

u', v', w'	Velocity fluctuations in x, y, and z-directions	(m/s)
$V_{i,j,k}$	V velocity at cell (i,j,k)	(m/s)
Δp	Pressure difference	(Pa)
α	Thermal diffusivity	(m^2/s)
β	Thermal expansion coefficient	(1/K)
ε	Turbulent energy dissipation rate	(m^2/s^3)
ρ	Density	(kg/m^3)
μ	Dynamic viscosity	(kg/m s)
υ	Kinematic viscosity	(m^2/s)
υt	Turbulent viscosity	(m^2/s)
σ_k, σ_ϵ	Constants for the k-ε model	

CHAPTER 1
INTRODUCTION

1.1 GENERAL INTRODUCTION

Indoor air quality (IAQ) and thermal comfort are the most important characteristics of the indoor environment. The heating, ventilation and air-conditioning systems, which can offer high IAQ and thermal comfort, have become more in present world. They can offer the sufficient amount of fresh or conditioned air to the occupied zone while effectively removing the contaminants and extra heat.

In the last several years, a growing body of scientific evidence has indicated that the air within homes and other buildings can be more seriously polluted than the outdoor air in even the largest and most industrialized cities. Other research indicates that people spend approximately 90 percent of their time indoors. Thus, for many people, the risks to health may be greater due to exposure to air pollution indoors than outdoors.

The temperature distribution and flow features within a room have a significant influence on health and thermal comfort of occupants. Thus the knowledge of flow and temperature fields is essential to heating, ventilation and air-conditioning (HVAC) engineers in order to design a good ventilation system.

In past the buildings were designed to be naturally ventilated. Therefore, it is normal that complaints about indoor air quality in non-industrial buildings have increased over the years. Parameters such as ventilation and pollution sources are documented as being of major importance. A healthy and pleasant climate is defined as a fairly low air velocity, small velocity and temperature gradients throughout the room, and also a low concentration of pollutants. A satisfactory distribution of ventilation-air in a room is essential to reach this aim. An unsatisfactory airflow pattern may be due to the lack proper air supply, temperature gradients within the room, type and positioning of supply and extract air-ducts, machines, furniture and other objects within a room. There are many configurations of ventilation air distribution systems and a wide range of potential conditions within residential or office buildings. The prediction of ventilation performance (and so indoor-environment quality) for any

specific situation is difficult. In fact, the required ventilation in a space depends on the total pollution source strength, the perceived air quality of the outdoor air, the desired perceived air quality and the ventilation efficiency in that space. The traditional way to determine the air quality in existing buildings is to ask people at their working place how they perceive the air. This procedure, as well as the experimental studies, is very time consuming and expensive. Computational fluid dynamics (CFD) makes it possible to simulate airflow patterns, thermal comfort and concentration distributions of pollutants in a space at much less cost.

1.2 NUMERICAL AND SIMULATION TECHNIQUES

The airflow in buildings involves a combination of most of the typical flow elements. The flow will always be incompressible and often turbulent due to the velocity levels and dimensions involved. Prediction of the distribution of velocity, temperature, and concentration in a room is not only available for designing air-condition systems.

Recent advancements in numerical methods for fluid–mechanics have been accompanied by investigations on numerical predictions of these distributions. However, in that case, because the air flow in a room is turbulent, one must apply the numerical methods in which the effects of turbulence on mean flow are taken into account.

The two equations closure turbulence models family is computationally reasonable and widely used. The standard k-ε model of Launder and Spalding is extensively used for the prediction of airflows in rooms and has also been used in the present study.

Because turbulent models are approximated methods, they need to be validated by experimental data before being used as a design tool. Some researchers have made effort to measure the airflows in the real rooms or use a small-scale model to represent a full-scale room. However, both experimental approaches are much more expensive than using the CFD technique and lack the flexibility to simulate various boundary conditions such as a complex diffuser. With the CFD techniques, whole field distribution can be obtained from solution, while in most experiments the measurements can only be carried out in a few locations of the room.

Nowadays, commercially available computational fluid dynamics codes (CFD codes) namely Fluent, CFX, phoenics are industrially used for a large range of applications, e.g. automotive industry, machinery, electronics and process industries. Present work uses CFD code Fluent in order to predict the indoor environment of a building room as such simulations can replace difficult and expensive experiments to asses the human comfort for various configuration.

CHAPTER 2

LITERATURE REVIEW

2.1 Computational Fluid Dynamics (CFD):

CFD is the systematic application of computing systems and computational solution techniques to mathematical models formulated to describe and simulate fluid dynamic phenomena.

CFD is the science of computing the motion of air, water, or any other gas or liquid. The CFD approach involves the numerical solution of a set of partial differential equations describing the fundamental laws of fluid motion. The solution of the discrete counterpart (algebraic system) of these equations provides values of velocities, temperatures, etc. at points or regions, rather than over the continuum. One of the most widespread approaches is the finite-volume method, which addresses the problem by subdividing the space (room) into a many subdomains where constant values of the properties are defined.

For incompressible flows, several methods exist to solve the algebraic systems of equations describing the physics of the air flow and heat transfer problem in the room. Undoubtedly, the classical one is the segregated approach, by means of which the various equations are tackled sequentially with the well-known pressures–velocity coupling algorithm (or its variants)

Computational fluid dynamics (CFD) solves fluid flow problems coupled with heat and mass transfers and turbulence phenomena in a given geometry by the use of a mesh where all the Navier–Stokes equations are solved across each mesh cell by means of an iterative procedure. When applying CFD to the IAQ and thermal comfort problem, the conservation of mass for a contaminant Species and energy for thermal responses also may be included. Due to the development of cheaper, more powerful computers and user-friendly commercial software packages, CFD techniques have been increasingly used in recent years in many areas.

2.1.1 Use of CFD

Knowing how fluids will flow, and what will be their quantitative effects on the solids with which they are in contact, assists:-

- Building-services engineers and architects to provide comfortable and safe human environments;
- Power-plant designers to attain maximum efficiency, and reduce release of pollutants;
- Chemical engineers to maximize the yields from their reactors and processing equipment;
- Land-, air- and marine-vehicle designers to achieve maximum performance, at least cost;
- Risk-and-hazard analysts, and safety engineers, to predict how much damage to structures, equipment, human beings, animals and vegetation will be caused by fires, explosions and blast waves.

2.1.2 The Strategy of CFD

Broadly, the strategy of CFD is to replace the continuous problem domain with a discrete domain using a grid. In the continuous domain, each flow variable is defined at every point in the domain. For instance, the pressure p in the continuous 1D domain shown in the figure below would be given as

$$p=p(x),\ 0<x<1; \tag{1}$$

In the discrete domain, each flow variable is defined only at the grid points. So, in the discrete domain shown in the Fig 2.1, the pressure would be defined only at the N grid points.

$$p_i = p\ (x_i),\ i=1,2,3\ \ldots\ldots N \tag{2}$$

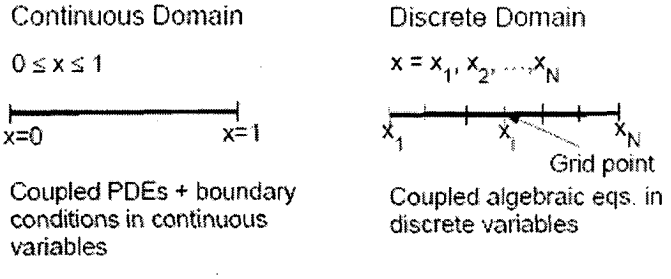

Fig 2.1 Continuous and discrete grid domains

In a CFD solution, one would directly solve for the relevant flow variables only at the grid points. The values at other locations are determined by interpolating the values at the grid points.

The governing partial differential equations and boundary conditions are defined in terms of the continuous variables p, $\vec{V}$ etc. One can approximate these in the discrete domain in terms of the discrete variables p_i, $\vec{V}$ etc. The discrete system is a large set of coupled, algebraic equations in the discrete variables. Setting up the discrete system and solving it (which is a matrix inversion problem) involves a very large number of repetitive calculations and is done by the digital computer.

2.1.3 Discretization Using the Finite-Difference Method

To illustrate the fundamental ideas underlying CFD, It is applied to the following simple one dimensional differential equation:

$$\frac{du}{dx} + u^m = 0; \qquad 0 \le x \le 1; \quad u(0) = 1 \tag{3}$$

first consider the case where m = 1 when the equation is linear.

Discrete representation of the above equation with m = 1 having four equally spaced grid points is shown on the following grid:

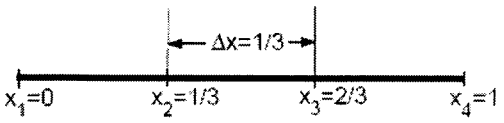

This grid has four equally-spaced grid points with Δx being the spacing between successive points. Since the governing equation is valid at any grid point, we have

$$\left(\frac{du}{dx}\right)_i + u_i = 0 \tag{4}$$

Using a first order backward difference to approximate the derivative terms of equation.

$$\frac{u_i - u_{i-1}}{\Delta x} + u_i = 0 \qquad \text{for i = 1,2,.....} \tag{5}$$

That is a differential equation is converted to an algebraic equation.

This method of obtaining the discrete equation is called the finite-difference method. However, most commercial CFD codes use the finite-volume or finite-element methods which are better suited for modeling flow past complex geometries.

2.1.4 Discretization Using the Finite-Volume Method

A close look at the airfoil grid shown earlier reveals that it consists of quadrilaterals. In the finite-volume method, such a quadrilateral is commonly referred to as a "cell" and a grid point as a "node". In 2D, one could also have triangular cells. In 3D, cells are usually hexahedrals, tetrahedrals, or prisms. In the finite-volume approach, the *integral form* of the conservation equations are applied to the control volume defined by a cell to get the discrete equations for the cell. For steady, incompressible flow, the integral form of continuity equation reduces to

$$\int_S \vec{V}.\hat{n}\,dS = 0 \qquad (6)$$

The integration is over the surface S of the control volume and $\hat{n}$ is the outward normal at the surface. Physically, this equation means that the net volume flow into the control volume is zero.

Consider the rectangular cell shown below.

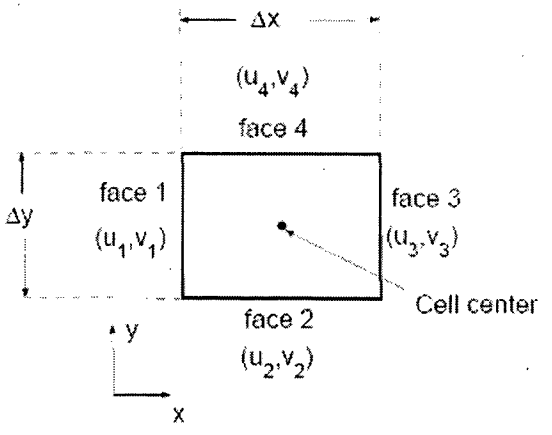

The velocity vector at face i is taken to be $\vec{V_i} = u_i\vec{i} + v_i\vec{j}$. Applying the mass conservation equation (6) to the control volume defined by the cell gives

$$u_1\Delta y + v_2\Delta x = u_3\Delta y + v_4\Delta x \qquad (7)$$

Rearranging Eq (7) the

$$-u_1\Delta y - v_2\Delta x + u_3\Delta y + v_4\Delta x = 0 \tag{8}$$

This is the discrete form of the continuity equation for the cell. It is equivalent to summing up the net mass flow into the control volume and setting it to zero. So it ensures that the net mass flow into the cell is zero i.e. that mass is conserved for the cell. Usually the values at the cell centers are stored. The face values u_1, v_2, etc. are obtained by suitably interpolating the cell-center values for adjacent cells.

Similarly, one can obtain discrete equations for the conservation of momentum and energy for the cell. One can readily extend these ideas to any general cell shape in 2D or 3D and any conservation equation.

2.2 FLUID DYNAMICS THEORY

This section outlines the basic fluid dynamic principles and equations relating to this project.

2.2.1 LAMINAR FLOW EQUATIONS

2.2.1.1 Conservation of Mass and Momentum:

If an Eulerian description is applied to a laminar flow field and constant density is assumed, the following continuity (conservation of mass) equation results.

$$\frac{\partial U}{\partial X_i}=0 \tag{9}$$

The conservation of momentum equations are given by

$$\frac{\partial U_i}{\partial t}+\frac{\partial}{\partial X_j}(U_iU_j)=-\frac{1}{\rho}\frac{\partial P}{\partial X_i}+g_i+\upsilon\nabla^2U_i \tag{10}$$

Where U_i, i=1, 2, 3, three components of the velocity vector.

2.2.1.2 Energy Equation:

If the conservation of energy is considered for a fluid engaged in laminar flow, the following equation represents the transport of heat within the flow field.

$$\frac{\partial T}{\partial t}+\frac{\partial}{\partial X_i}(U_iT)=\alpha(\nabla^2T) \tag{11}$$

2.2.2 MODELS FOR TURBELENCE FLOW:

The air movement in a ventilated room often is turbulent. The air flows in buildings involve a combination of many different flow elements. It is, therefore, difficult to find an adequate, all-round turbulence model covering all aspects. Consequently, it is appropriate and economical to choose turbulence models according to the situations that is to be predicted.

The standard k-ϵ model of Launder and Splading[1974] is extensively used for the prediction of air flows in rooms. Many modifications have been made to this first model:

A k-ϵ model expanded by damping functions is used to improve the prediction of the flow in a room ventilated by displacement ventilation .The damping functions

Zero-Equation model:

The turbulence is described through the use of algebraic equations. Thus the only partial differential equations requiring solution are the mean flow continuity and momentum equations.

A simple zero-equation model can be used for the prediction of special situations as flow with a low level of turbulence.

One-Equation model:

A partial differential equation for the turbulence velocity scale is solved in addition to the mean flow partial differential equation

Two-Equation model (Three-Dimensional):

Two partial differential equations for the turbulent velocity fields scales are solved in addition to the mean flow equations. Even though there are numerous models which may be employed, this study makes use of a two-equation model

2.2.2.1 Turbulent Flow Equations

The velocity components in turbulent flow are

$$\begin{aligned} U &= \overline{U} + u' \\ V &= \overline{V} + v' \\ W &= \overline{W} + w' \end{aligned} \tag{12}$$

2.2.2.2 Equation of continuity

If the velocity expressions of Eq(12) are substituted into the continuity equation of Eq(9), the following equation results after a time average is taken.

$$\frac{\partial \overline{U_i}}{\partial X_i} = 0 \quad \text{for i=1,2,3.....} \tag{13}$$

2.2.2.3 Equation of Momentum

If the velocity expressions of Eq(12) are substituted into the momentum equation, Eq(10), and a time average is taken, the following equation will result.

$$\frac{\partial \overline{U_i}}{\partial t} + \frac{\partial}{\partial X_j}(\overline{U_i U_j}) + \frac{\partial}{\partial X_j}(\overline{U_i' U_j'}) = -\frac{\partial}{\partial X_i}\left(\frac{P}{\rho}\right) + g_i + \upsilon \nabla^2 \overline{U_i} \tag{14}$$

Eq (14) may be manipulated slightly to distinguish the right-hand side of the equation as containing both viscous and turbulent (Reynolds) stresses as shown by the following equation.

$$\rho \frac{\partial \overline{U_i}}{\partial t} + \rho \frac{\partial}{\partial X_j}(\overline{U_i U_j}) = -\frac{\partial P}{\partial X_i} + \rho g_i + \frac{\partial}{\partial X_j}(\mu \frac{\partial \overline{U_i}}{\partial X_j}) + \frac{\partial}{\partial X_j}(-\rho \overline{u_i' u_j'}) \tag{15}$$

The fact that these Reynolds stresses consist of correlations of velocity fluctuations render the stresses impossible to solve. This incapacity to predict the correlations is known as the "Closure Problem." As a result, exact solutions are not possible.

2.2.3 k- ε Turbulence Model

k-ϵ turbulence model is used to numerically simulate the turbulence model. This model has been widely applied in predicting many types of turbulent flow phenomena. It is a two equation model which couples equations for the turbulent kinetic energy (k) and the turbulence dissipation rate (ϵ). The mathematics of the model begin by defining the turbulent kinetic energy as

$$k = \frac{1}{2}\overline{u_i u_j} \tag{16}$$

The Reynolds stresses are then modeled by the product of a new term, the turbulent viscosity (υ_t), and the mean velocity gradient as shown by

$$\overline{u_i u_j} = \upsilon_t\left(\frac{\partial U u_i}{\partial X_j} + \frac{\partial U_j}{\partial X_i} - \frac{2}{3}k\delta_{ij}\right) \tag{17}$$

Where $\delta_{ij} = 1$ for i = j

$=0$ for i $\neq$ j

If this new expression for the Reynolds stresses is substituted into the momentum equation, the following new equation may be used as the conservation of momentum equation for turbulent flow. Note that the viscous stress is assumed negligible and that the equation is now coupled with the turbulent kinetic energy.

$$\frac{\partial U_i}{\partial t} + \frac{\partial}{\partial X_j}(U_i U_j) = \frac{\partial}{\partial X_j}\left(\frac{P}{\rho}\right) + g_i + \frac{\partial}{\partial X_j}\left(\upsilon_t\left(\frac{\partial U_i}{\partial X_j} + \frac{\partial U_j}{\partial X_i}\right) - \frac{2}{3}k\delta_{ij}\right) \tag{18}$$

This turbulent viscosity term (υ_t) is not a property of the fluid in the same way as the Newtonian viscosity. Rather, it is dependent upon the structure of the turbulence in the flow and may differ at various points throughout the flow. The turbulent viscosity may be determined empirically from Eq(19), although it is only one of several possible choices for the turbulent viscosity equation.

$$\upsilon_t = C_\mu \frac{k^2}{\varepsilon} \tag{19}$$

Where C_μ=0.09

The resulting transport equations for the turbulent kinetic energy and its rate of dissipation are shown in the following equations. Again, it must be emphasized that only a very brief summary of this model is being presented. Further detail may be found in Rodi [1980] or Hinze [1987],

$$R_e = \frac{U_o L_0}{\upsilon} \tag{20}$$

$$\frac{\partial \varepsilon}{\partial t} + \frac{\partial}{\partial X_j}(U_j \varepsilon) = \frac{\partial}{\partial X_j}\left(\frac{\upsilon_t \partial \varepsilon}{\sigma_\varepsilon \partial X_j}\right) + \frac{C_1 \upsilon_t \varepsilon}{k}\frac{\partial U_i}{\partial X_j}\left(\frac{\partial U_i}{\partial X_j} + \frac{\partial U_j}{\partial X_i}\right) - C_2\frac{\varepsilon^2}{k} \tag{21}$$

Though intermediate steps in the derivation of Eq(20) and Eq(21) result in the presence of higher order correlations. The unsolvable nature of these correlations is alleviated by modeling the correlations in the equations. The recommended values of

the empirical constants and functions are given in the Table 2.1. These values represent what is considered the "standard" k-ε model.

Table 2.1 Constants for the standard k-ϵ model

C_0	C_1	C_2	σ_1	σ_2	σ_3
0.09	1.44	1.92	1.0	1.3	1.0

Justification for k-ε Use:

Launder and Spalding's[1974] two-equation k-ε model is probably the most extensively used and validated model employed for turbulent fluid dynamics. The broad use of the model over the has highlighted both its capabilities and shortcomings. The model has achieved notable success when dealing with thin shear layers and recirculating flows without the need for case-by-case modification of the model constants. Also model success is noted when simulating confined flow phenomena where the normal Reynolds stresses are somewhat insignificant compared to the Reynolds shear stresses which are of utmost importance.

The model is favored for industrial applications due to its fairly low computational expense and generally better numerical stability than more complex higher order turbulence models such as the Differential Stress Equation Model (DSM) pioneered by Launder et, al., [1972]

The model's popularity also reduces the implementation difficulty since there are several references available discussing the numerical aspects of modeling turbulence through the use of the k-ε equations. Because the k-ε model is a two-equation model, improved accuracy is obtained in comparison to less-complicated models. Researchers investigating some of the primary two-equation models have discovered that only the k-ε model yields experimentally substantiated results for regions far from solid boundaries or walls [Launder, 1974; Launder, et al., 1972]. For the other models to match the results, it was found necessary to replace some of the constants with empirical functions which added to the complexity of the models.

2.2.4 Low-Reynolds Number Model

Several authors have devised turbulence model equation which is valid throughout the laminar, semi-laminar, fully turbulent regions. The recommendations of Jones and Launder are summarized here; they extended the k-ϵ model to low Reynolds number flows.

When discussing turbulent flow, it is convenient to mention an additional parameter, the Turbulent Reynolds Number (R_T)

$$R_T = \frac{k^2}{\varepsilon \upsilon} \tag{22}$$

Due to the nature of room air flow, there will always be regions (particularly near the walls) in which this number is quite small. In these regions, the viscous effects become significantly greater than any turbulent effects. Because the standard form of the k-ε model is valid only for high Reynolds number turbulent flows, difficulty arises. There are two ways in which the fully turbulent k-ε model may be used for low-Reynolds number flow. These methods are known as wall functions and low-Reynolds models.

The wall functions, when used in conjunction with the standard k-ε equations, are intended to reproduce the logarithmic velocity profile of a turbulent boundary layer near the wall. No changes are made to the k-ε equations. Instead, the velocity profile is created through the use of complex expressions imposed as boundary conditions at the walls. Although a detailed derivation and explanation is not included, following equations number Eq(23) through Eq(26) represent wall functions introduced by Launder and Spalding [1974]. It is important to note in the following equations that values with the "wall" subscript (w) denote values at the wall, while values of, U_t, k and ε are values at the first node adjacent to the wall.

$$\frac{U_t}{\tau_w / \rho}(C_\mu^{\frac{1}{2}} k)^{1/2} = \frac{1}{k}\ln\left(\frac{E y_n (C_\mu^{1/2} k)^{1/2}}{\upsilon}\right) \tag{23}$$

$$\left(\frac{\upsilon_t}{\sigma_k}\frac{\partial k}{\partial y_n}\right)_{wall} = 0 \tag{24}$$

$$\varepsilon^* = \frac{(C_\mu^{1/2}k)^{\frac{3}{2}}}{ky_n}\ln\left(\frac{Ey_n(C_\mu^{\frac{1}{2}}k)^{\frac{1}{2}}}{\upsilon}\right) \tag{25}$$

$$\varepsilon = \frac{(C_\mu^{\frac{1}{2}}k)^{\frac{3}{2}}}{ky_n} \tag{26}$$

Where k = von Karman's constant (0.4).

τ_w = shear stress at the wall.

E = function determined by wall roughness (9.0 for a smooth wall).

ε^* =value of ε used in the k-equation.

ε = value of ε used in the ε-equation

Wall functions have the significant benefits of reducing computational needs as well as allowing the addition of other empirical functions necessary for special boundary conditions. The primary concern with this method is that the high-Reynolds k-ε model with the logarithmic wall functions may not be suitable for use both near the wall and far away from it [Chen, 1990]. In addition, the traditional wall functions may not be appropriate for complex three-dimensional flow.

The second method for describing low-Reynolds number flow involves modifying the standard k-ε equations, making them valid throughout the full range of flow regions (laminar, buffer, and fully turbulent). Changes are made through the addition of the empirical functions Fμ, F1, F2, and E, as shown in the following low-Reynolds equations.

$$\frac{\partial k}{\partial t} + \frac{\partial}{\partial X_j}(U_j k) = \frac{\partial}{\partial X_j}\left(\frac{\upsilon_t}{\sigma_k}\frac{\partial k}{\partial X_j}\right) + \upsilon_t \frac{\partial U_i}{\partial X_j}\left(\frac{\partial U_i}{\partial X_j} + \frac{\partial U_j}{\partial X_i}\right) - \varepsilon \tag{27}$$

$$\frac{\partial \varepsilon}{\partial t} + \frac{\partial}{\partial X_j}(U_j \varepsilon) = \frac{\partial}{\partial X_j}\left(\frac{\upsilon_t}{\sigma_\varepsilon}\frac{\partial \varepsilon}{\partial X_j}\right) + \frac{C_1 F_1 \upsilon_t \varepsilon}{k}\frac{\partial U_i}{\partial X_j}\left(\frac{\partial U_i}{\partial X_j} + \frac{\partial U_j}{\partial X_i}\right) - C_2 F_2 \frac{\varepsilon^2}{k} + E \tag{28}$$

$$\upsilon_t = C_\mu F_\mu \frac{k^2}{\varepsilon} \tag{29}$$

$$R_T = \frac{k^2}{\upsilon\varepsilon} \tag{30}$$

$$R_y = \frac{\sqrt{k}}{\upsilon} y_n \tag{31}$$

Where y_n = distance normal to the wall (m)

The table 2.2 contains the various empirical constants for three of the more popular low-Reynolds number k-ε models. For comparison, values are also given for the standard, high-Reynolds number model.

Table 2.2 Low-Reynolds k-ε constants [Patel, 1984]

Model	C_μ	C_1	C_2	σ_k	σ_ϵ
Standard	0.09	1.44	1.92	1.0	1.3
Launder-Sharma	0.09	1.44	1.92	1.0	1.3
Chien	0.09	1.35	1.8	1.0	1.3
Lam-Bremhorst	0.09	1.44	1.92	1.0	1.3

The table 2.3 contains the values and expressions for the empirical functions which have been added to the original k-ε equations to model low-Reynolds number flow.

Table 2.3 Low-Reynolds k-ε functions [Patel, 1984]

Model	F_μ	F_1	F_2	E
standard	1	1	1	0
Launder-sharma	$\exp(\frac{-3.4}{(1+\frac{R}{50})^2})$	1	$1-0.3\exp(-R_t^2)$	$2\nu\nu_t(\frac{\partial^2 u}{\partial y_n^2})^2$
Chien	$1-\exp(-0.0115y^+)$	1	$1-0.22\exp(-(R_T/6)^2)$	$\frac{-2\nu\varepsilon}{y^2}\exp(-0.5y^+)$
Lam - Bremhorst	$[1-\exp(-0.0165R_y)]^2 * (1+\frac{20.5}{R_T})$	$1+(\frac{0.05}{F_\mu})^3$	$1-\exp(-R_t^2)$	0

The "standard" k-ε model for fully turbulent flow is a special case of the low-Reynolds equations of Eq(27) and Eq(28). Therefore, a solution algorithm could

easily employ the wall function or low-Reynolds algorithms by simply using the corresponding values of, $F\mu$ F_1, and F_2.

Low Reynolds number models (LRN models) are used to improve the prediction of evaporation-controlled emissions from building material. This model is very suitable for the prediction of mass and energy transfer coefficients at surfaces. This model predicts the transport processes in the laminar sub-layer and the log-law zone in contrast to the standard k- ϵ model where this part of the flow is given by analytical wall functions.

2.2.5 LARGE EDDY SIMULATION

The velocity field with in a room is described by the equations of continuity and momentum. In large eddy simulation, any physical quantity f is decomposed in to two parts:

$$f = \bar{f} + f'' \tag{32}$$

Here, $\bar{f}$ is the resolvable –scale component and f'' is the subgrid-scale component. $\bar{f}$ is defined with a filter function G(X,Y) as follows:

$$\bar{f}(X) = \iiint G(X,Y) f(Y) dY \tag{33}$$

Here, a top-hat filter function is used as G(X,Y),

$$G(X,Y) = \left\{ \prod_{I=1}^{3} \frac{1}{\Delta_I} \right\} \qquad |x - y_i| \le \frac{1}{2}\Delta_i \tag{34}$$

$$= 0 \qquad |x_i - y_i| > \frac{1}{2}\Delta_i$$

Where Δ_i is the component grid size in the x_i direction, X, Y is a position vector.

Imposing function (33) on eq (9), eq(10) filtered equations are given as follows:

$$\frac{\partial \overline{U_i}}{\partial X_i} = 0 \tag{35}$$

$$\frac{\partial \overline{U_i}}{\partial t} + \frac{\partial \overline{U_i U_J}}{\partial x_j} = -\frac{1}{\rho}\frac{\partial \bar{p}}{\partial x_i} + \frac{\partial}{\partial x_j}\left[\overline{-U_I'' U_j''} - \overline{U_I'' \bar{U}_j} - \overline{\bar{U}_I U_j''} - \left(\overline{\bar{U}_I \bar{U}_j} - \overline{U_I U_j} \right) + \nu \frac{\partial \overline{U_I}}{\partial x_j} \right] \tag{36}$$

In this study, Reynolds averaging assumption is applied:

$$\overline{\bar{U}_I \bar{U}_j} - \overline{U_I U_j} + \overline{U_I'' \bar{U}_j} + \overline{\bar{U}_i U_j''} = 0 \tag{37}$$

Then we get

$$\frac{\partial \overline{U_i}}{\partial t} + \frac{\partial \overline{U_I U_j}}{\partial x_j} = \frac{\partial p^*}{\partial x_i} + \frac{\partial}{\partial x_i}\left[-\left(\overline{-U_I^{"} U_j^{"}} - \frac{1}{3}\overline{-U_I^{"} U_i^{"}}\delta_{ij} \right) + \nu \frac{\partial \overline{U_i}}{\partial x_j} \right] \tag{38}$$

Where $p^* = \frac{p}{\rho} + \frac{1}{3}\overline{U_I^{"} U_I^{"}}$

Here, Reynolds number is assumed to be very large so that the viscous term can be neglected. The viscous sublayer at the wall is not treated explicitly. In eq (38), $\overline{U_i}$ and p^* are variables whose values are computed at mesh points of the computational fluid.

2.3 OTHER MODELS

This section presents brief descriptions of the published literature and recorded experimental results in the field of room air flow modeling and prediction. Although the list should not be considered exhaustive, the review should sufficiently represent the advances, findings, and contributions which are of particular relevance to this project.

Spitler

The experimental data used for comparative purposes in this project has been provided by Spitler [1990]. Spitler researched air movement and convective heat transfer using a full-scale 9 x 9 x 15 ft (2.74 x 2.74 x 4.57 m) room with 53 controllable heated panels, two ventilation inlets, and one outlet (see Figure 2.2). The facility incorporated sixteen omni-directional air speed probes and numerous thermocouples which measured air temperatures within the room, air temperatures entering and leaving the room, and the various surface temperatures necessary in determining the convective fluxes at the walls. These probes obtained measurements at 896 locations within the room, thus providing an experimental grid of approximately 1 ft (0.30 m). Experimental data was collected using the seven rooms configuration described in table 2.4.

Table 2.4 Experimental configurations.

EXPERIMENTAL CONFIGURATIONS
[Spitler. 1990]

Configuration	Description
1	One inlet on the side wall
2	One square radial diffuser inlet in the ceiling
3	The side wall inlet with area reduced to 1/3
4	The side wall inlet with area reduced to 2/3
5	The side wall inlet with its jet being diverted toward the center of the room
6	The side wall inlet with furniture located in the center of the room
7	The side wall inlet with cabinets located throughout the room

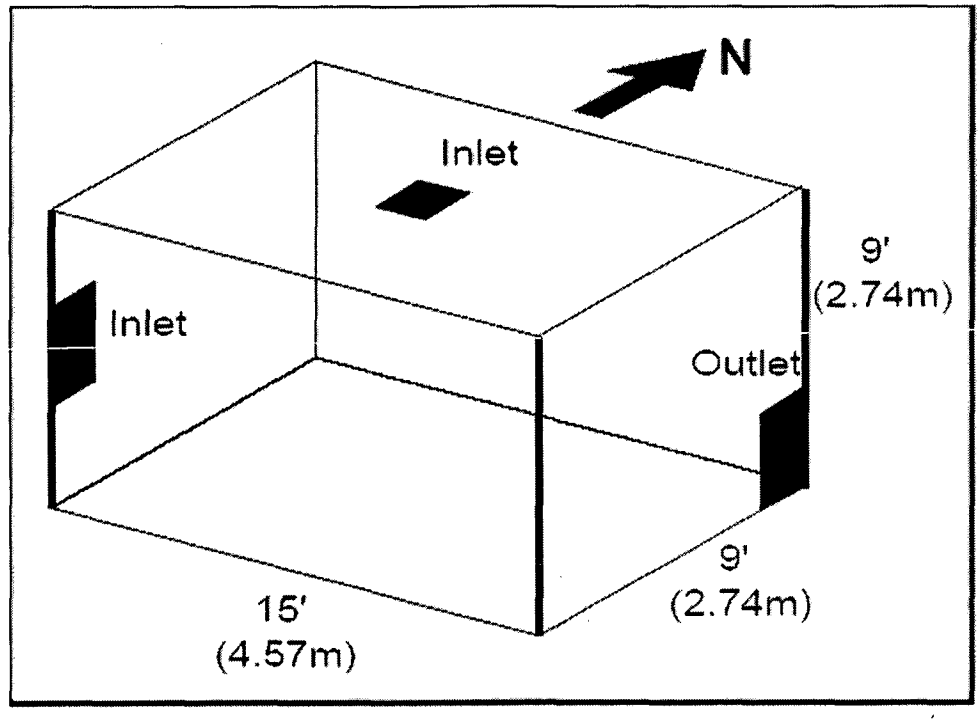

Fig 2.2 Experimental facility
[spitler 1990]

In all of the room configurations, one ventilation outlet located on the east wall was used (see Figure 2.2). The dimensions of the inlets and outlets are shown in Table 1.5. With the presentation of Table 1.5, it is important to note how inlet dimensions are generally used in room air flow studies to define non-dimensional parameters and distances. Throughout this report, dimensional distances are presented. In addition, results will be presented by defining distances with respect to the inlet width. Thus, y/W=2 would correspond to a distance equal to twice the inlet width.

Table 2.5 Inlet and outlet dimensions.

INLET AND OUTLET DIMENSIONS
[Spitler, 1991]

Location	Width (in)	Length (in)	Width (m)	Length (m)
Side Wall Inlet	15.75	35.58	0.40	0.90
Ceiling Inlet	15.75	15.75	0.40	0.40
East Outlet	15.75	35.58	0.40	0.90

The ventilation system was capable of providing between 2 and 100 ACH ("air changes per hour") of ventilation. This corresponds to volumetric flow rates of 40.5 -2025 cfm (0.019 - 0.945 m3/s). A total of 44 separate experimental tests were performed, as described in Table 1.6. The use of the 53 controllable panels is of particular interest to the modeling aspect of this study. By controlling the temperature of the walls, the convective heat fluxes were measured and film coefficients for all surfaces were calculated. This data allows the imposition of temperature boundary conditions which are consistent with experimental data.

Table 2.6 Experimental tests.

EXPERIMENTAL TESTS
[Spitler, 1991]

Configuration	Inlet Temperature (°C)	Ventilation Rate (ACH)
1	16, 21, 26	15, 30, 50, 70, 100
2	16, 21, 26	15, 30, 50, 70, 100
3	21	15, 30, 50, 70
4	21	15, 30, 70
5	21	15, 30, 70
6	21	30, 70
7	21	30, 70

Patel

An extensive review of the k-ε model for low Reynolds number flow was compiled by Patel [Patel, 1985]. In addition to the nature and derivation of the model, Patel also detailed the following seven variations or extensions of the model:

1. Launder-Sharma
2. Hassid-Poreh
3. Hoffman
4. Dutoya-Michard

5. Chien

6. Reynolds

7. Lam-Bremhorst

In an attempt to compare the models, each model was implemented with the addition of the following equations to numerically predict flow in a two-dimensional boundary layer.

$$\frac{\partial U}{\partial X}+\frac{\partial V}{\partial Y}=0 \tag{39}$$

$$U\frac{\partial U}{\partial X}+V\frac{\partial U}{\partial Y}=-\frac{1}{\rho}\frac{\partial P}{\partial X}+\frac{\partial}{\partial Y}\left(\upsilon\frac{\partial U}{\partial Y}-\overline{UV}\right) \tag{40}$$

The proposed models of Hassid-Poreh, Hoffman, Dutoya-Michard, and Reynolds failed to reproduce the simple case of this flat-plate boundary layer. Comparable results to experimental data were achieved through the use of the Launder-Sharma, Chien, and Lam-Bremhorst models. Despite these successful results, a refinement to the models was determined necessary if near-wall and low Reynolds number flows were to be calculated.

Patel offered the following suggestions:

1. Select a damping function for the shear stress which is in agreement with experimental evidence.

2. Choose the low Reynolds number functions in the dissipation rate equation with a mathematically consistent near-wall behavior.

3. "Fine tune" the functions to ensure that well-published features of wall bounded shear flows over a range of pressure gradients would be produced.

4.Distinct improvement of the predictions for adverse pressure gradient flows would require additional modifications to the high Reynolds number models.

Lam and Bremhorst

Since the emergence of the k-ε turbulence model, numerous researchers have introduced modifications to the basic models, particularly in an attempt to accurately predict low-Reynolds number turbulent flow. Perhaps one of the more significant modifications was introduced by Lam and Bremhorst [Lam & Bremhorst, 1981]. As

with the previous models, the turbulent energy and its dissipation rate were modeled using Eq(27) and (28). The constants being used were the same as the original model: σ_K=1.0, σ_ε =1.3, C_μ=0.09, C_1=1.44, and C_2=1.92.

The primary difference exists in the functions F_μ, F_1, and F_2 in the low-Reynolds equations of Eq(27) and Eq(28). Previously, the values of these functions were assumed to be equal, or very close to unity. The research of Lam and Bremhorst found these assumptions to be invalid within a laminar or viscous sub layer. A new equation for Fμ was found to be

$$F_\mu = (1-\exp(-A_\mu R_y))^2\left(1+\frac{A_t}{R_t}\right) \tag{41}$$

Where $A_\mu = 0.0165$ $A_t = 20.5$

This new equation is directly influenced by the presence of a wall, as Fμ will approach unity at large distances from a wall for increasingly high levels of turbulence

The proposed equation for F1 was

$$F_1 = 1+\left(\frac{0.05}{F_\mu}\right)^3 \tag{42}$$

Investigation showed that if F_1 was equal to unity, as previously assumed, additional terms would be required in the k-ε equations to yield reasonable results. In an effort to produce an equation which approaches zero as R_T approaches zero, the following equation for F2 was introduced.

$$F_2 = 1-\exp(-R_T^2) \tag{43}$$

This new low-Reynolds form of the k-e model was tested by applying the technique to the case of fully developed turbulent pipe flow. Strong agreement was found with the experimental data. The principle advantage, as emphasized by the researchers, is that the presence of a wall function formula is not required.

Chen

As discussed earlier, one of the particular difficulties with modeling room air flow is that the k-ε model, although suitable for fully turbulent flow, requires the use of empirical functions near the wall. Chen explored the wall function problem as he attempted to accurately prediction low-Reynolds, turbulent, buoyant flow [Chen, 1990]. Chen used the Lam-Bremhorst version of the k-ε model [Lam & Bremhorst, 1981] to predict natural convection flow within cavities. This version of the model was chosen based on recommendations by previous researchers [Patel, 1985] and its relative ease of implementation into a computer algorithm. It was assumed that any temperature gradients within the cavity were small, therefore the use of Boussinesq approximation for buoyancy was performed through the addition of the following term in the momentum equations.

$$\beta g_i (T - T_o) \tag{44}$$

The effects of buoyancy in the turbulence equations were approximated using the following terms in the k-ε equations.

$$S_k = \frac{\beta \upsilon_t}{\sigma_h} \frac{\partial}{\partial X_i} (T - T_o) g_i \tag{45}$$

$$S_\varepsilon = \frac{1.44 \varepsilon S_k}{k} \tag{46}$$

These source terms would then be included in the right-hand side of Eq(27) and Eq(28)

The first of the two simulations was performed on a small-scale, water-filled cavity. The second simulation was made on a full-scale, air filled cavity. The resulting velocity profiles were in good agreement with the measured values. However, the high-Reynolds number k-ε model with wall functions produced results which differed by as much as 61% from the experimental results.

Awbi

Perhaps the most significant application of CFD analysis in room air flow may be in the area of ventilation. Studies have shown that the thermal condition within a room is dependent on the turbulence intensity of the air motion and frequency of flow fluctuations, in addition to the air velocity and temperature distributions. Awbi

presented numerical studies of various ventilation configurations through the use of CFD [Awbi, 1989].

Using the standard k-ε model, coupled with logarithmic wall functions, simulations were performed on the ventilation of both two and three-dimensional enclosures. Other simulations involved creating a fixed or constant load within the room to better investigate the effects of buoyancy. The numerical solutions produced reasonably good predictions of the velocity vectors within the room when compared to experimental results. Awbi carefully noted, though, that considerably more studies are necessary if CFD techniques are to be used as design tools with any degree of confidence.

Murakami, et al.

Murakami, et al. from the University of Tokyo, have contributed greatly to the study of numerically modeling room air flow. Each study has emphasized different facets of the overall problem, thus providing a better insight concerning the potential for CFD in ventilation design and analysis.

The first investigations were performed with the intention of verifying the validity of a three-dimensional numerical simulation for turbulence [Murakami, et al., 1987]. Simulations were performed and compared to experimental rooms with a 1:6 scale. The experimental rooms were scaled so that the Reynolds number would be identical to a full scale room based on the following equation.

$$R_e = \frac{U_o L_0}{\upsilon} \tag{47}$$

Where U_0 = inlet velocity (m/sec)

L_0 = width of supply outlet (m)

The flow domain was covered with a rectangular mesh. Later investigations employed the use of boundary-fitted curvilinear coordinate systems [Murakami, et al., 1989a]. The air temperature was assumed to be completely uniform. Thus, buoyant effects were completely ignored. The high-Reynolds k-ε equations Eq(20) and Eq(21) were solved in conjunction with the momentum equation of Eq(18). The standard values for the equation constants were used and wall functions were used to simulate viscous effects near the wall.

The numerical simulations were reported to correspond "fairly good" with the experimental results from the scaled room. Later investigations focused on the diffusion of particles within a ventilated room, with particular emphasis on the design and analysis of clean rooms [Murakami, et al., 1989b, 1990]. The same sets of equations and wall functions were used to analyze other scaled room configurations. Scaling the room based on the inlet velocity and inlet width is questionable when investigating turbulent room air flow. Scaling in this way does not insure identical turbulent Reynolds numbers. In addition, the development of turbulent jets is based on other parameters which are completely independent of the Reynolds number at the inlet.

2.4 Air movement in naturally- ventilated buildings [Wrec, 1996]

Natural ventilation is now considered to be one of the requirements for a low energy building design. Until about three decades ago the majority of office buildings in the UK were naturally ventilated. With the availability of inexpensive fossil energy and the tendency to provide better indoor environmental control, there has been a vast increase in the use of air-conditioning in new and refurbished buildings. However, recent scientific evidence on the impact of refrigerants and air-conditioning systems on the environment has prompted the more conscious building designers to give serious considerations to natural ventilation in non-domestic buildings.

Two major difficulties that a designer has to resolve are the questions of air-flow control and room air movement in the space. In mechanically ventilated spaces, there are well established techniques for assessing the air movement that a system is expected to produce.

Because of the problem of scaling and the difficulty of representing natural ventilation in a laboratory, most of the methods used for predicting the air movement in mechanically ventilated buildings are not very suitable for naturally ventilated spaces. Computational fluid dynamics (CFD) is becoming increasingly used for the design of both mechanical and natural ventilation systems. Since a CFD solution is based on the fundamental flow and energy equations, the technique is equally applicable to a naturally ventilated space and a mechanically ventilated space providing that a realistic representation of the boundary conditions are made in the solution.

2.4.1 Flow equations

Wind

The volume flow rate (Q) through a large opening is given by:

$$Q=C_dA\sqrt{\frac{2\Delta p}{\rho}} \tag{48}$$

where C_d is the discharge coefficient, A is the area, ρ is the density and Δp is the pressure difference which is given by:

$$\Delta p = 0.5\ \rho\ V_r\ C_p \tag{49}$$

where V_r is the reference wind speed and C_p is the pressure coefficient at the opening. For a number of openings in parallel:

$$C_dA = \sum(C_d\ A)_i \tag{50}$$

and for a number of openings in series:

$$\frac{1}{(C_dA)^2} = \sum\frac{1}{(C_dA)_i^{\ 2}}$$

Buoyancy

The volume flow rate through a large opening due to temperature difference is given by

$$Q = \frac{C_d}{3}\sqrt{\frac{gH\Delta T}{\overline{T}}} \tag{51}$$

where ΔT is the temperature difference across the opening and $\overline{T}$ is the mean temperature (K).

CHAPTER 3

MODEL AND MODEL EQUATIONS

A flow field can be described by the conservation of mass, momentum and energy. Given the boundary conditions, the resulting flow pattern is determined by solving the combined Navier-Stokes and energy or any other scalar equations.

3.1 MATHEMATICAL MODEL:

3.1.1 CONTINUITY EQUATION:

$$\frac{\partial}{\partial x_1}(u_1) = 0 \tag{52}$$

$$\frac{\partial}{\partial x_2}(u_2) = 0 \tag{53}$$

$$\frac{\partial}{\partial x_3}(u_3) = 0 \tag{54}$$

3.1.2 MOMENTUM BALANCE:

$$\frac{\partial}{\partial t}(u_1) + \frac{\partial}{\partial x_1}(u_1 u_1) = -\frac{\partial}{\partial x_1}\left(\frac{p}{\rho} + \frac{2}{3}k\right) + \frac{\partial}{\partial x_1}\left[\vartheta_t\left(\frac{\partial}{\partial x_1}(u_1) + \frac{\partial}{\partial x_1}(u_1)\right)\right] \tag{55}$$

$$\frac{\partial}{\partial t}(u_1) + \frac{\partial}{\partial x_2}(u_1 u_2) = -\frac{\partial}{\partial x_1}\left(\frac{p}{\rho} + \frac{2}{3}k\right) + \frac{\partial}{\partial x_2}\left[\vartheta_t\left(\frac{\partial}{\partial x_2}(u_1) + \frac{\partial}{\partial x_1}(u_2)\right)\right] \tag{56}$$

$$\frac{\partial}{\partial t}(u_1) + \frac{\partial}{\partial x_3}(u_1 u_3) = -\frac{\partial}{\partial x_1}\left(\frac{p}{\rho} + \frac{2}{3}k\right) + \frac{\partial}{\partial x_3}\left[\vartheta_t\left(\frac{\partial}{\partial x_3}(u_1) + \frac{\partial}{\partial x_1}(u_3)\right)\right] \tag{57}$$

$$\frac{\partial}{\partial t}(u_2) + \frac{\partial}{\partial x_1}(u_2 u_1) = -\frac{\partial}{\partial x_2}\left(\frac{p}{\rho} + \frac{2}{3}k\right) + \frac{\partial}{\partial x_1}\left[\vartheta_t\left(\frac{\partial}{\partial x_1}(u_2) + \frac{\partial}{\partial x_2}(u_1)\right)\right] \tag{58}$$

$$\frac{\partial}{\partial t}(u_2) + \frac{\partial}{\partial x_2}(u_2 u_2) = -\frac{\partial}{\partial x_2}\left(\frac{p}{\rho} + \frac{2}{3}k\right) + \frac{\partial}{\partial x_2}\left[\vartheta_t\left(\frac{\partial}{\partial x_2}(u_2) + \frac{\partial}{\partial x_2}(u_2)\right)\right] \tag{59}$$

$$\frac{\partial}{\partial t}(u_2) + \frac{\partial}{\partial x_3}(u_2 u_3) = -\frac{\partial}{\partial x_2}\left(\frac{p}{\rho} + \frac{2}{3}k\right) + \frac{\partial}{\partial x_3}\left[\vartheta_t\left(\frac{\partial}{\partial x_3}(u_2) + \frac{\partial}{\partial x_2}(u_3)\right)\right] \tag{60}$$

$$\frac{\partial}{\partial t}(u_3) + \frac{\partial}{\partial x_1}(u_3 u_1) = -\frac{\partial}{\partial x_3}\left(\frac{p}{\rho} + \frac{2}{3}k\right) + \frac{\partial}{\partial x_1}\left[\vartheta_t\left(\frac{\partial}{\partial x_1}(u_3) + \frac{\partial}{\partial x_3}(u_1)\right)\right] \tag{61}$$

$$\frac{\partial}{\partial t}(u_3)+\frac{\partial}{\partial x_2}(u_3u_2)=-\frac{\partial}{\partial x_3}\left(\frac{p}{\rho}+\frac{2}{3}k\right)+\frac{\partial}{\partial x_2}\left[\vartheta_t\left(\frac{\partial}{\partial x_2}(u_3)+\frac{\partial}{\partial x_3}(u_2)\right)\right] \quad (62)$$

$$\frac{\partial}{\partial t}(u_3)+\frac{\partial}{\partial x_3}(u_3u_3)=-\frac{\partial}{\partial x_3}\left(\frac{p}{\rho}+\frac{2}{3}k\right)+\frac{\partial}{\partial x_3}\left[\vartheta_t\left(\frac{\partial}{\partial x_3}(u_3)+\frac{\partial}{\partial x_3}(u_3)\right)\right] \quad (63)$$

3.1.3 TRANSPORT EQUATION FOR k:

$$\frac{\partial}{\partial t}(k)+\frac{\partial}{\partial x_1}(ku_1)=\frac{\partial}{\partial x_1}\left(\frac{\vartheta_t}{\sigma_1}\frac{\partial}{\partial x_1}k\right)+\vartheta_t s-\varepsilon \quad (64)$$

$$\frac{\partial}{\partial t}(k)+\frac{\partial}{\partial x_2}(ku_2)=\frac{\partial}{\partial x_2}\left(\frac{\vartheta_t}{\sigma_1}\frac{\partial}{\partial x_2}k\right)+\vartheta_t s-\varepsilon \quad (65)$$

$$\frac{\partial}{\partial t}(k)+\frac{\partial}{\partial x_3}(ku_3)=\frac{\partial}{\partial x_3}\left(\frac{\vartheta_t}{\sigma_1}\frac{\partial}{\partial x_3}k\right)+\vartheta_t s-\varepsilon \quad (66)$$

3.1.4 TRANSPORT EQUATION FOR ε

$$\frac{\partial}{\partial t}(\varepsilon)+\frac{\partial}{\partial x_1}(\varepsilon u_1)=\frac{\partial}{\partial x_1}\left(\frac{\vartheta_t}{\sigma_2}\frac{\partial}{\partial x_1}\varepsilon\right)+C_1\frac{\varepsilon}{k}\vartheta_t s-C_2\frac{\varepsilon^2}{k} \quad (67)$$

$$\frac{\partial}{\partial t}(\varepsilon)+\frac{\partial}{\partial x_2}(\varepsilon u_2)=\frac{\partial}{\partial x_2}\left(\frac{\vartheta_t}{\sigma_2}\frac{\partial}{\partial x_2}\varepsilon\right)+C_1\frac{\varepsilon}{k}\vartheta_t s-C_2\frac{\varepsilon^2}{k} \quad (68)$$

$$\frac{\partial}{\partial t}(\varepsilon)+\frac{\partial}{\partial x_3}(\varepsilon u_3)=\frac{\partial}{\partial x_3}\left(\frac{\vartheta_t}{\sigma_2}\frac{\partial}{\partial x_3}\varepsilon\right)+C_1\frac{\varepsilon}{k}\vartheta_t s-C_2\frac{\varepsilon^2}{k} \quad (69)$$

$\vartheta_t = k^{0.5}l = C_0k^2/\varepsilon$

$\sigma_1 = 1.0 \qquad C_0 = 0.09$

$\sigma_2 = 1.3 \qquad C_1 = 1.44$

$C_2 = 1.92$

$$s=\left(\frac{\partial}{\partial x_j}(u_i)+\frac{\partial}{\partial x_i}(u_j)\right)\frac{\partial}{\partial x_j}(u_i) \quad (70)$$

3.2 BOUNDARY CONDITIONS

The equations described in the above section are solved to predict the air velocity and temperature distribution in mechanically ventilated (heated or cooled) rooms. Since the boundary conditions are unique to a particular flow situation, an accurate representation of these conditions is necessary for a reliable solution to be achieved. For the ventilated rooms it is necessary to specify the conditions as inlet, outlet and on the internal surfaces of the room. In general three types of boundary conditions are used.

3.2.1 INLET CONDITION:

Uniform distribution is used over the inlet boundary of the longitudinal velocity, u_o, temperature, T, kinetic energy of turbulence, k, and the energy dissipation rate, ε. Other quantities such as pressure and the other two velocity components are taken as zero at the inlet.

The kinetic energy of turbulence is calculated using

$$k = (3/2)\, I^2 u_o^2 \tag{71}$$

Where I^2 is the turbulence intensity of the u-component of velocity at the inlet which is taken as 0.14 in the absence of measured values,

The dissipation rate is obtained from

$$\varepsilon = k^{1.5} / (\lambda H) \tag{72}$$

Where λ is a constant taken as 0.005 and H is the room height or the square root of the cross sectional area of the room.

3.2.2 OUTLET CONDITIONS:

The longitudinal component of velocity u_e is derived from the continuity equation, i.e

$$u_e = u_o \frac{A_o}{A_e} \frac{\rho_o}{\rho_e} \tag{73}$$

and the other velocity components and the pressure are assumed to be zero. The exit temperature T_e is obtained from the energy equation for the whole flow field taking into account heat transfer across all boundaries. Boundary conditions for k and ε are not required because an up-wind computational scheme, is used expect that their gradients in the exit plane are zero. Uniform distribution of u_e and T_e is assumed across the exit area.

3.2.3 WALL BOUNDARY

Close to a wall region laminar viscosity becomes more significant than turbulent viscosity as a result of the damping effect of the wall, i.e $\frac{\partial}{\partial y}(k) = 0$ at the wall. So the turbulence model equations do not apply to regions close to a solid boundary and instead the wall-function equations due to Launder and Spalding are used for the velocity component parallel to the boundary. With in the laminar sublayer region viscous effects pre-dominate and the wall shear stress, τ_w, is described by the usual couette flow expression. At a point outside this region turbulent shear becomes significant and it can be shown that when the generation and dissipation of energy is in balance then

$$\frac{\tau}{\rho} = C_{\mu}^{0.5} k \tag{74}$$

The boundary temperatures can be specified to represent the actual temperatures of the room surfaces or to represent the temperature of a heat source or a sink of a known capacity. Heat fluxes or sinks can be treated as additional source terms in the energy equation.

CHAPTER 4

NUMERICAL SIMULATION

The problem is to create a room shape having one inlet, two windows on side walls of the room, and two exhausts on opposite walls to inlet, and two exhausts on ceiling wall of the room.

The same size room is used in two models , difference is on the operating temperatures used.

Model 1 is the room of having walls at the same temperature.

Model 2 is the same room, but walls are maintained at different temperatures.

4.1 Development of Geometric model 1:

The dimensions of room are

Length: 6 m

Width: 6 m

Height: 4.5 m.

The inlet door is of rectangular shape of having width of 1.5 m and height of 2.5 m.

The inlet is placed in front wall of the room at z=2.25m.

Windows are of rectangular shape of having 2 m. and height of 1 m. The windows are placed in side walls at x = 2 m ,y=1 m and x=2 m, y=1 m, z=6 m.

Exhausts are of circular shape having radius of 0.5 m.

The exhausts on opposite wall of inlet are at x = 6 m , z = 1 m and at x = 6 m , z = 5 m. These are at height of 3 m.

The exhausts on top wall are at x = 2 m and z=1.5 m and at x =2 m and at z = 4.5 m.

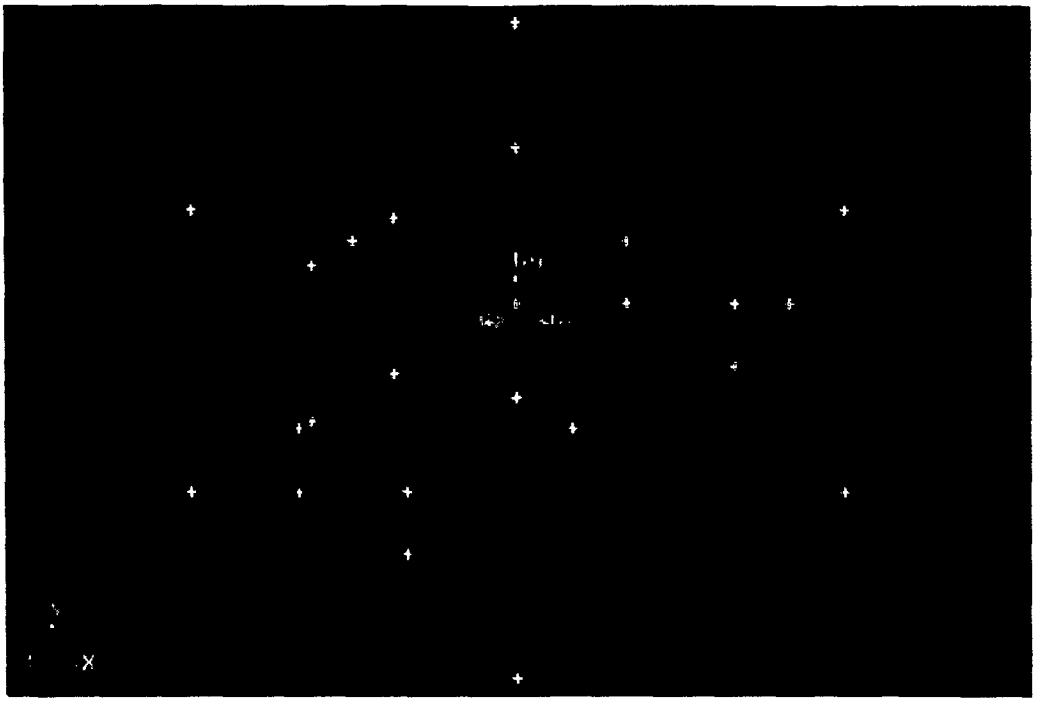

Fig 4.1 Isometric view

4.2 MESH GENERATION

Meshing Scheme used:

Elements chosen: Tet

The Elements parameter defines the shape of the elements that are used to mesh the volume. Tet specifies that the mesh includes only tetrahedral elements.

Type chosen: Hex Core

Type parameter defines the meshing algorithm and therefore, the overall pattern of mesh elements in the volume. Hex Core algorithm sweeps the mesh node patterns of specified source faces through the volume.

Specifications of Meshing of the geometry

Air volume:

Elements : Tet

Type : Hex core

Interval size : 0.5 m

Smoothing scheme used: Length-weighted Laplacian

This scheme uses the average edge length of the elements surrounding each node.

Boundary conditions

Boundary conditions specify the flow and thermal variables on the boundaries of the physical model.

Symmetry boundary conditions are used when the physical geometry of interest, and the expected pattern of the flow / thermal insulation, have mirror symmetry. Table 4.1 gives the boundary types of the room used.

Table 4.1 Boundary type

Face Position	Name	Type
Left face, Right face, Bottom face, Top face, Front face, Back face (excluding subfaces)	walls	WALL
Left sub face	Inlet 1	VELOCITY_INLET
Front subface	Inlet 2	VELOCITY_INLET
Back subface	Inlet 3	VELOCITY_INLET
Right subfaces	Exhausts 1	EXHAUST_FAN
Top subfaces	Exhaust 2	EXHAUST_FAN

Continuum specified

Fluid: volume of air inside room

Solid: All boundary walls

The generated meshed model is as shown in fig 4.5.

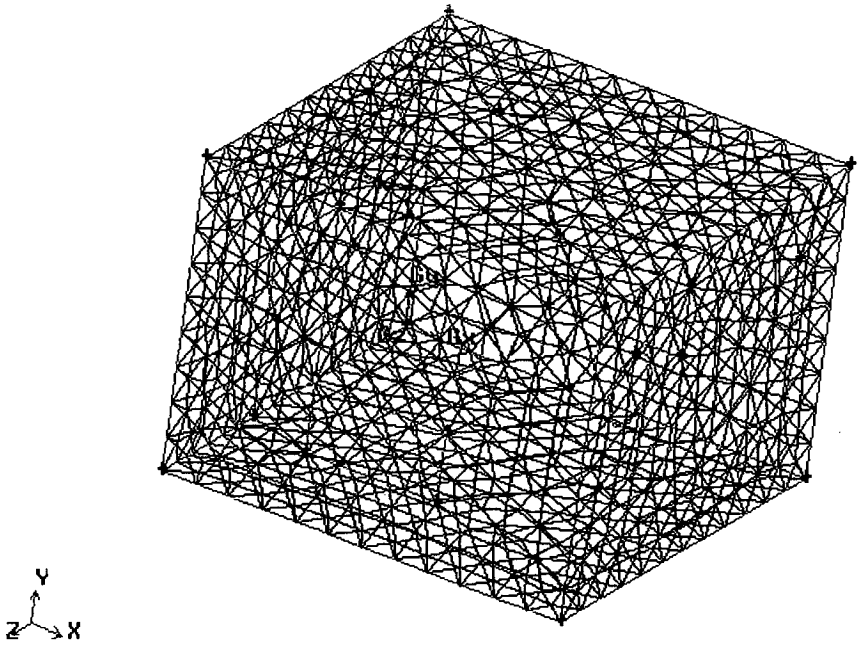

Fig 4.2 Meshing geometry

ZONING:

In the created volume all the boundaries and inside volumes and inlets outlets are labeled as shown in Fig 4.3

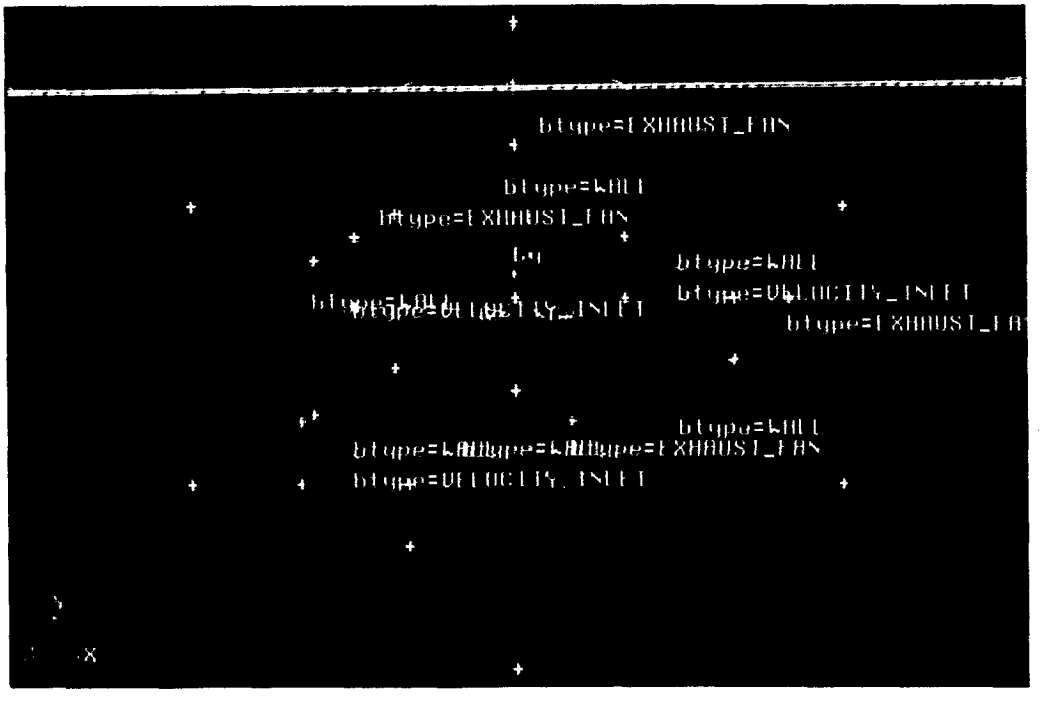

Fig 4.3 Labeled geometry

4.3 SOLUTION PROCESS

The mesh file is read in Fluent 6.2.16 solver. In solving the problem the following steps are involved.

Import Grid

Grid check, Grid scaling and Grid Display

After reading the mesh file, grid checking has been done to make sure that there are no errors. Any errors in the grid would be reported at this time. Then scaling of the grid is done.

Defining the models , Materials and conditions of Model 1

Models: Solver

Segregated solver is the solution algorithm by which the governing equations are solved sequentially.(i.e., segregated from one another). Steady state 3-Dimensional solver is considered.

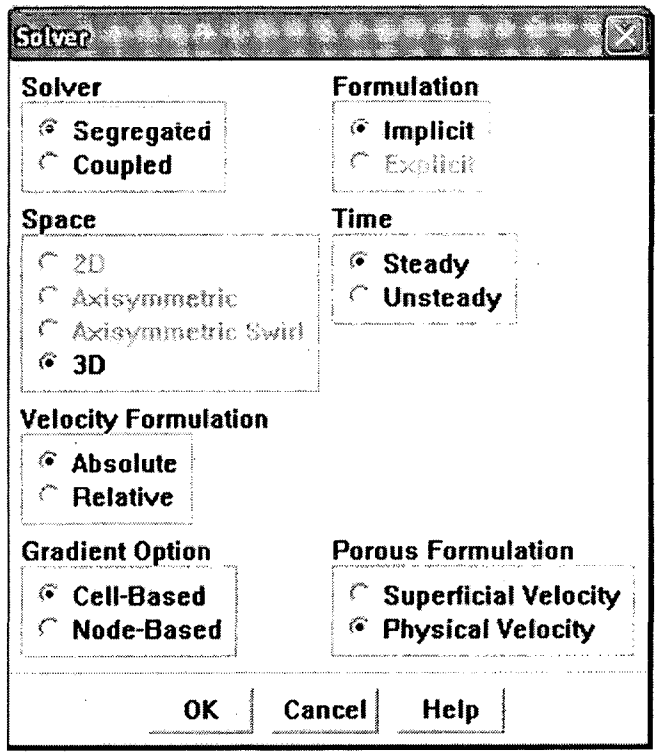

Fig 4.4 Solver panel.

Other models choosen : Energy

Viscous

Under viscous model, turbulent model is selected, because in this problem the flow field would be turbulent. Here K-ε turbulent model has been e used.

Defining material properties:

For concrete and air the properties have been taken from the FLUENT database. Air properties are at normal temperature and pressure (atmospheric conditions)

Table 4.2 Properties of air.

Density	1.225	kg/ m^3
Specific heat	1006.43	J/kg-K
Thermal conductivity	0.0242	W/m-k
Viscosity	0.00001789	kg/m-s

Concrete properties are at normal temperature and pressure (atmospheric conditions)

Table 4.3 Properties of concrete

Density	2400	kg/ m^3
Specific heat	885	J/(kg K)
Thermal conductivity	242	W/(m k)

Defining operating conditions :

Operating pressure : 101325 Pa

Gravity : -9.81 m/s^2 (as it is in –y direction)

Defining boundary conditions

Here boundary conditions of inlets, wall, exhausts, default, and fluid interior are defined. In this model the walls are set at the same temperature normally at 300K.This is the main assumption for this model.

Table 4.4 Boundary conditions of wall.

Zone name	Type	Boundary conditions	
Walls	WALL	Wall thickness	0.25 m
		Heat flux	0 W/ m^2
		Heat generation rate	0 W/ m^3

This set of boundary conditions is used for all walls.

Table 4.5 Boundary conditions of inlet

Zone name	Type	Boundary conditions	
Inlet 1	VELOCITY_INLET	Velocity magnitude	1 m/s
		Temperature	300 K
		Turbulence specification method	k-ε model
		Turbulent kinetic energy	1 m^2/s^2
		Turbulence dissipation rate	1.2 m^2/ s^3

This set of boundary conditions is used for all inlets.

Table 4.6 Boundary conditions of Exhaust.

Zone name	Type	Boundary	
Exhaust 1	EXHAUST_FAN	Gauge pressure	0.3 bar
		Temperature	300 K
		Turbulence specification method	k-ε model
		Turbulent kinetic energy	1 m^2/s^2
		Turbulence dissipation rate	1.2 m^2/ s^3

This set of boundary conditions is used for all exhaust fans.

Convergence criterion :

The convergence for the variables is defined in the following table.

Table 4.7 Convergence criterion.

Variable	**Convergence criterion**
Continuity	0.001
X- velocity	0.001
Y- velocity	0.001
Z- velocity	0.001
Energy	1e-06

Solution Initialization and Iterations

Solution is initialized and number of iterations assigned is 300. The solution is not converged within the given iterations; number of iterations is increased to 500.Then the solution gets converged in 382 iterations.

4.4 Development of Geometric model 2 :

The dimensions of model 2 are same as in model 1.

4.5 MESH GENERATION

Meshing Scheme used:

Elements choosen : Tet

The Elements parameter defines the shape of the elements that are used to mesh the volume. Tet specifies that the mesh includes only tetrahedral elements.

Type choosen : Hex Core

Type parameter defines the meshing algorithm and therefore, the overall pattern of mesh elements in the volume. Hex Core algorithm sweeps the mesh node patterns of specified source faces through the volume.

Specifications of Meshing of the geometry

air volume :

Elements : Tet

Type : Hex core

Interval size : 0.5 m

Smoothing scheme used : Length-weighted Laplacian

This scheme uses the average edge length of the elements surrounding each node.

Boundary conditions

Boundary conditions specify the flow and thermal variables on the boundaries of the physical model.

Wall boundary conditions are used to bound fluid and solid zones.

Face Position	Name	Type
Left face, Right face, Bottom face, Top face, Front face, Rear face (excluding subfaces)	walls	WALL
Left subface	Inlet 1	VELOCITY_INLET
Front subface	Inlet 2	VELOCITY_INLET
Rear subface	Inlet 3	VELOCITY_INLET
Right subfaces	Exhausts 1	EXHAUST_FAN
Top subfaces	Exhaust 2	EXHAUST_FAN

Continuum specified

Fluid: volume of air inside room

Solid: All boundary walls

4.6 SOLUTION PROCESS

The mesh file is read in Fluent 6.2.16 solver. In solving the problem the following steps are involved.

Import Grid

Grid check, Grid scaling and Grid Display

After reading the mesh file, grid checking has been done to make sure that there are no errors. Any errors in the grid would be reported at this time. Then scaling of the grid is done. Grid size can be seen through grid size panel.

Defining the models, Materials and conditions of Model 2

Models: Solver

Segregated solver is the solution algorithm by which the governing equations are solved sequentially.(i.e., segregated from one another). Steady state 3-Dimensional solver is considered

Other models choosen : Energy

Viscous

Under viscous model, turbulent model is selected, because in this problem the flow field would be turbulent. Here K-ε turbulent model has been e used. Results are displayed for this turbulent model.

Defining boundary conditions

Here the boundary conditions are same as for the model 1 except wall temperatures. In this model walls are set at different temperatures as mentioned below.

Zone name	Type	Boundary conditions	
Walls	WALL	Wall thickness	0.25 m
		Heat flux	0 W/ m^2
		Heat generation rate	0 W/ m^3

Table 4.8 Boundary conditions of wall temperature.

Wall	Temperature
Left wall	305 K
Right wall	310 K
Front wall	305 K
Back wall	315 K
Top wall	315 K
Ground wall	305 K

Discretization schemes and convergence criteria is also same as in the case of model 1.

Solution Initialization and Iterations

Solution is initialized and number of iterations assigned is 300. The solution is not converged within the given iterations; number of iterations is increased to 500.Then the solution gets converged in 363 iterations.

CHAPTER 5

RESULTS AND DISCUSSIONS

In this chapter results of model 1 and model 2 presented and discussed. Modelling and simulations of the model given in Chapter 4 is carried out with CFD package FLUENT 6.2.16. Modelling of these models is done according to the equations given in Chapter 3, and simulations are carried out according the simulation techniques give in Chapter 4. These were performed on P4 CPU based PC. In FLUENT 6.2.16, the creation of geometry and meshing is done in GAMBIT and specification of operating and boundary condition is done in FLUENT. Iterations are carried out with the convergence criteria given in Table 4.7.

5.1 RESULTS AND DISCUSSIONS OF MODEL 1

In model 1 all the walls were set at same temperature of 300 K. The temperature distribution is uniform through out the room. Velocity profiles and contours of velocity are obtained for different inlet velocities. Contours of pressure are obtained for different gauge pressures.

The results obtained below are using k-ε turbulence model for inlet velocity of 1m/s and sucking gauge pressure of exhausts is 0.3 bar. The convergence criterion is as given in Table 4.7. The solution gets converged at 382 iterations.

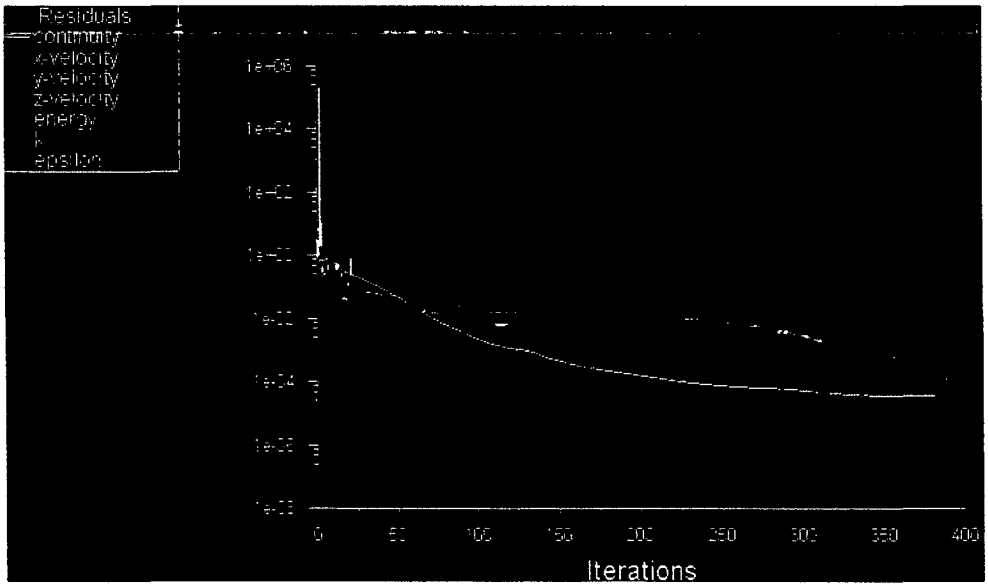

Fig 5.1 Scaled residuals

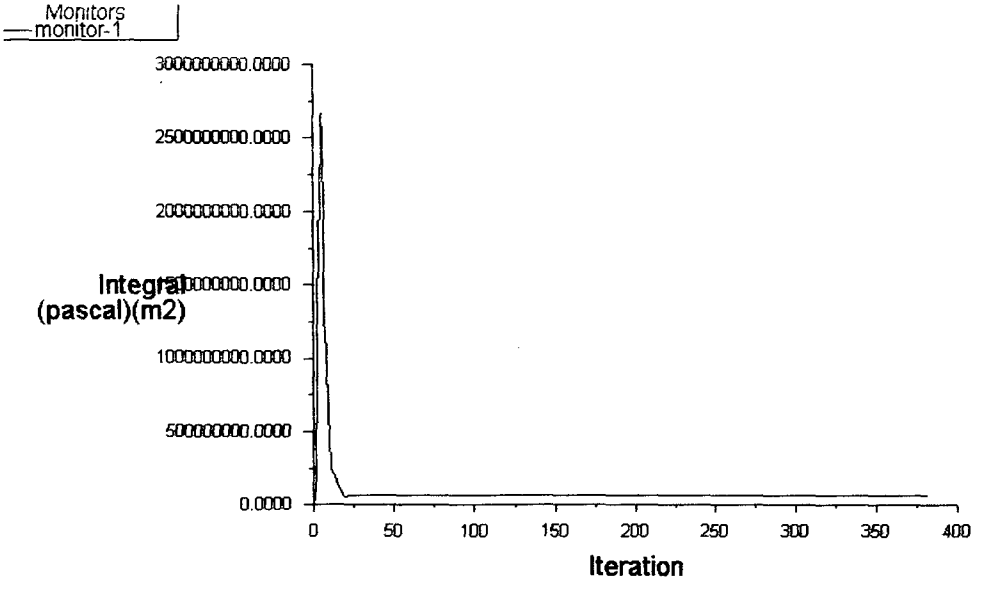

Fig 5.2 Convergence history of static pressure on interior of model 1.

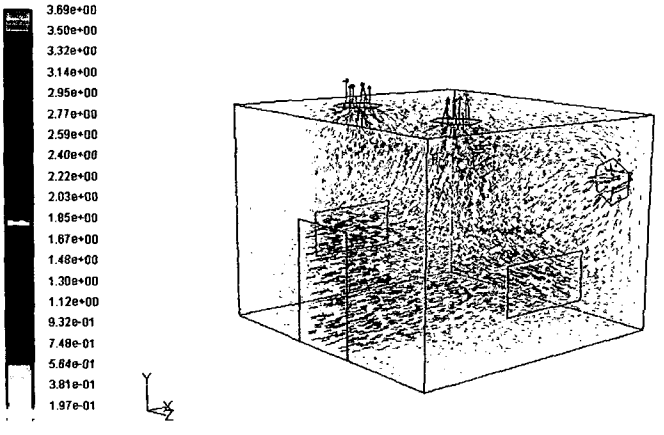

Fig 5.3 Velocity vectors colored by velocity magnitude (m/s)

Fig 5.3, shows the velocity vectors colored by velocity magnitude in room in three dimensional views. The maximum velocity is at exhausts i.e. 0.36 m/s, and the velocity is high also at inlet and windows. The air coming from the inlet and from windows is sucked by the exhausts on ceiling and right wall of the room.

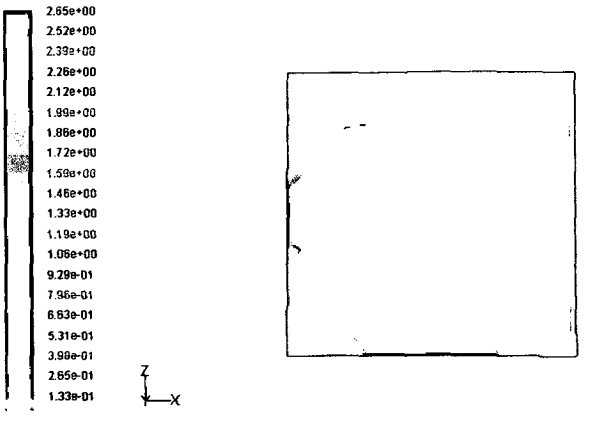

Fig 5.4 Contours of velocity magnitude (m/s) at y = 2 m

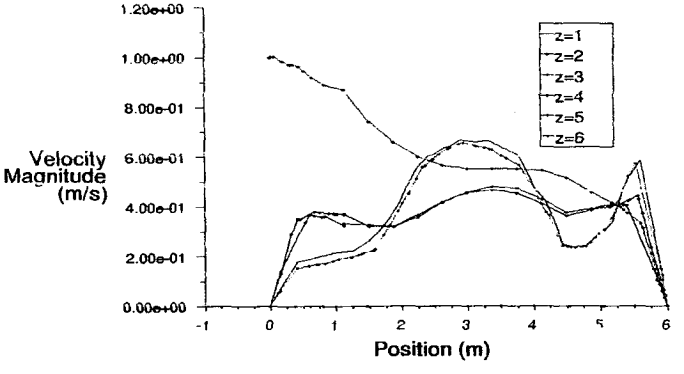

Fig 5.5 Velocity plots at y=2 m along the length of the room.

It is clear from Fig 5.4 and Fig 5.5, that the velocity is high at a height of y= 2 m, and at x=0 and z=3 i.e. 1 m/s, because inlet is located at z=2.25 m, velocity is high at the middle part of the inlet. The velocity at the windows is also high, having high value adjacent to the window i.e. 1 m/s. The velocity is having minimum value at the corners of the room i.e. 0.33 m/s. The velocity in the room is between 0.265 m/s and 0.663 m/s. The velocity is at the exhausts (at x=5.5 m) is also having high value i.e.0.663 m/s.

The velocity at x=0 and z=1 m, z=2 m, z=4 m, z=5 m, z=6 m is zero, velocity is increasing along the length of the room and becoming maximum at around x=3 m, this velocity increase is due to windows. The velocity is becoming zero at x= 6m.

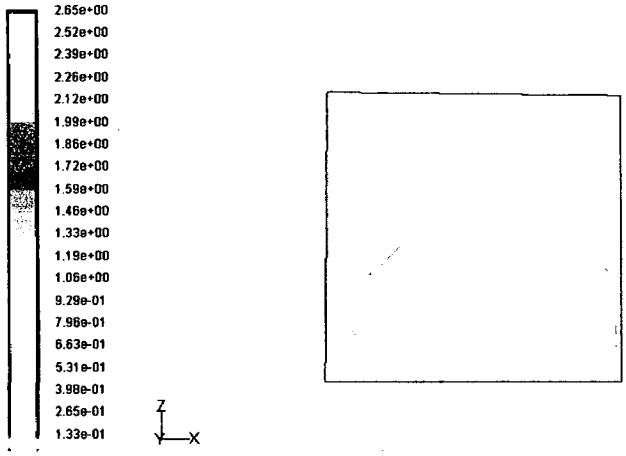

Fig 5.6 Contours of velocity magnitude (m/s) at y = 4 m

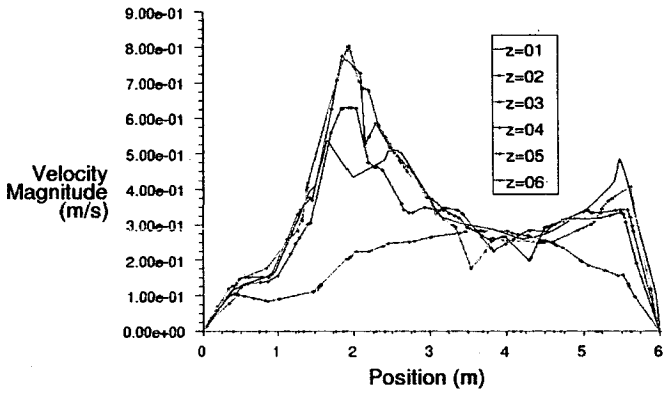

Fig 5.7 Velocity plots at y=4 m along the length of the room

From Fig 5.6, Fig 5.7 the velocity at height of y= 4 m and at z=0 is 0 m/s. The velocity is high value at the middle of the exhaust at z= 3 m i.e. 0.85 m/s. The average velocity within the room is 0.25 m/s. Again the velocity is 0 m/s at the corners.

The velocity increase is due to exhausts on the ceiling of the room, the velocity is decreasing from x= 2 m to x= 5 m, again the velocity is increasing between x=5 m and x=6 m and becoming zero at x= 6 m. The velocity increase between x= 5 m and x= 6 m is due to the exhausts on right wall. The velocity at z= 6m is zero along the length of the room.

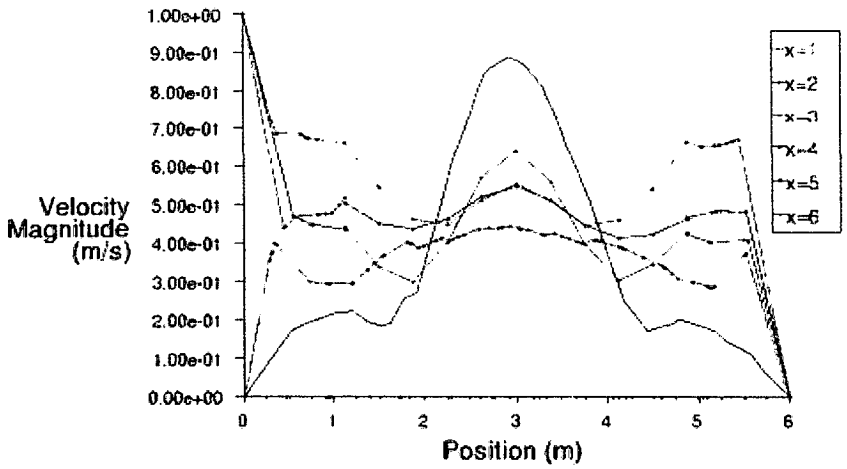

Fig 5.8 Velocity plots at y=2 m along width of the room

From Fig 5.8 the velocity at x=2 m and z =0 m ,at x=3 m and z=0 m, at x = 4 m and z= 0 m is maximum due to the window on back wall of the room, this velocity is decreasing up to z= 2 m, then increasing to maximum at z=3 m due to inlet, again the velocity is decreasing up to z= 5 m and increasing between z= 5 m and z= 6 m due to the effect of window on front wall of the room. The velocity at x= 6m along the width of the room is zero. The velocity at x=1 m and z= 0 m, at x=5 m and at z= 0 m is zero, this velocity is increasing to maximum at z=3 due to the effect of inlet and then decreasing to zero at z=6 m.

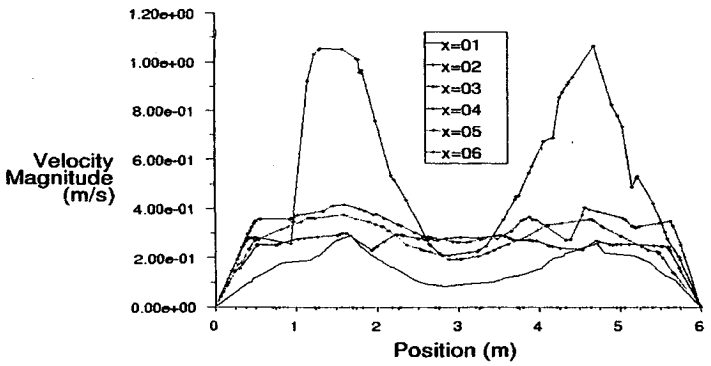

Fig 5.9 Velocity plots at y= 4 m along width of the room

From Fig 5.9 the velocity x= 1 m, x= 2 m, x= 3 m, x=4 m, x= 5 m, x= 6 and at z=0 m is zero due no effect of windows, inlets and windows, but the velocity at x=2 m, z=1.5

m and at x=2 m, z=4.5 is becoming maximum due to the effect of exhausts on ceiling of the room. The velocity for all values of x is becoming zero at z=6 m.

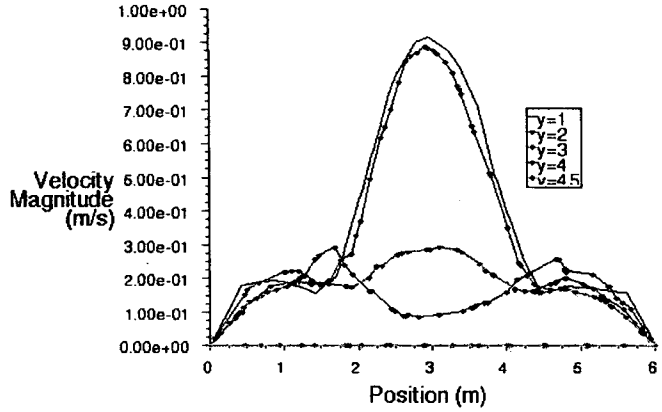

Fig 5.10 Velocity plots at x=1 m along the width of the room

From Fig 5.10the velocity at y=1 m, y=2 m, y= 3 m, y= 4 m, y= 4.5 and at z=0 m is zero, the velocity at y= 1 m , z=3 m and at y= 2 m, z=3 m is maximum due to the effect of inlet. The velocity for all values of y is becoming zero at z= 6 m. There is little effect of inlets and windows at y= 3 m, y=4 and y=4.5 m along width of the room.

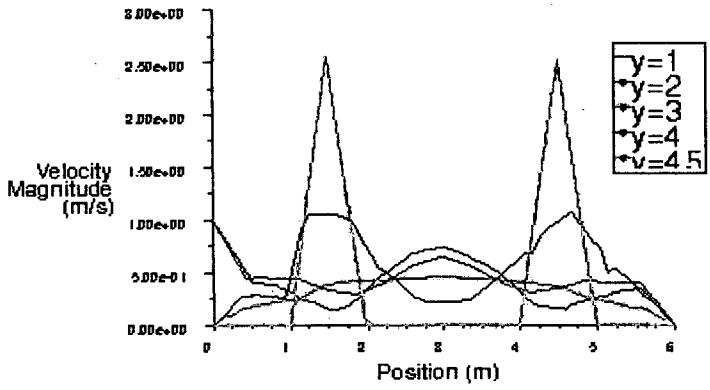

Fig 5.11 Velocity plots at x=2 m along the width of the room

From Fig 5.11 the velocity at y=4.5 m between z=0 m and z= 1m is zero and is increasing to maximum between z= 1m and z= 2 m, and between z= 4 m and z=5 m due to effect of exhausts on the ceiling of the room. The velocity at y=1 m ,z=0 m and at y= 2 m, z=0 is 1 m/s and is decreasing gradually ,then increasing between z= 2 m

and z= 4 m due to effect of exhausts on ceiling of the room, then decreasing gradually to zero at z= 6 m. There is low velocity at y= 3 m along the width of the room.

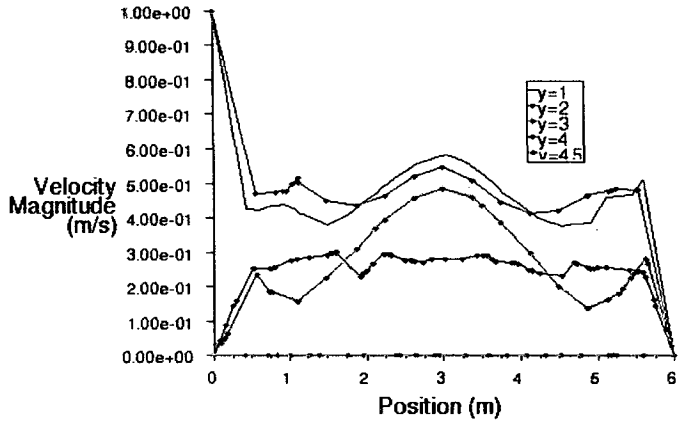

Fig 5.12 Velocity plots at x=4 m along the width of the room

From Fig 5.12 the velocity at y=2 m, z= 0 m and y=1 m, z=0 is 1 m/s, this velocity is decreasing up to z= 2 m and then increasing to maximum at z= 3 m due the effect of inlet and windows. The velocity at z= 0 m, y=3 m and z=0 m, y=4 m is zero. The velocity at y=3 m is gradually increasing and decreasing between z= 0 and 1 m and then increasing to maximum at z= 3 m, then decreasing till z= 5 m and then increasing and becoming zero at z= 6m. The velocity at y=4.5 m is zero along the width of the room.

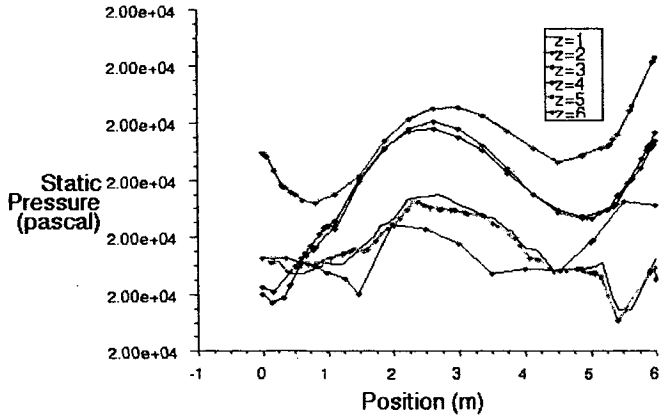

Fig 5.13 Plots of pressure at y=1 along the length of the room.

From Fig 5.13 pressure for all values of z is increasing to maximum between x= 2 m and x= 3 m this is due the effect of inlet and windows, the pressure is decreasing between x= 3 m and x=5 m, an d then increasing to maximum at x= 6 m. The maximum pressure at x=6 m is due the exhausts on right wall.

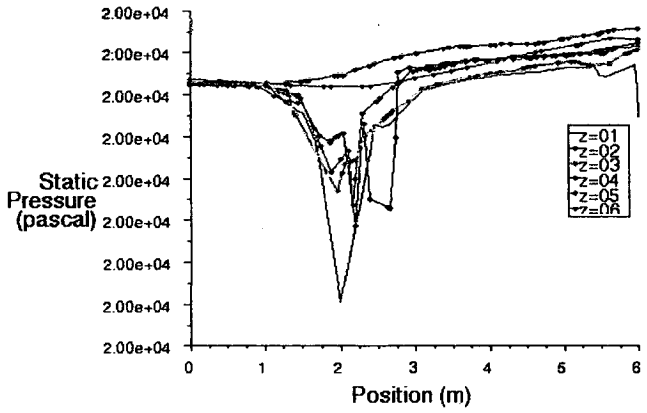

Fig 5.14 Plots of pressure at y=4 along the length of the room.

From Fig 5.12 pressure at x= 0 m is 20000 Pa for all values of z. The pressure at z= 3 m is increasing along the length of the room. The pressure for remaining values of z is decreasing to minimum between x=2 m and x= 3 m ,and increasing gradually until x= 6 m.

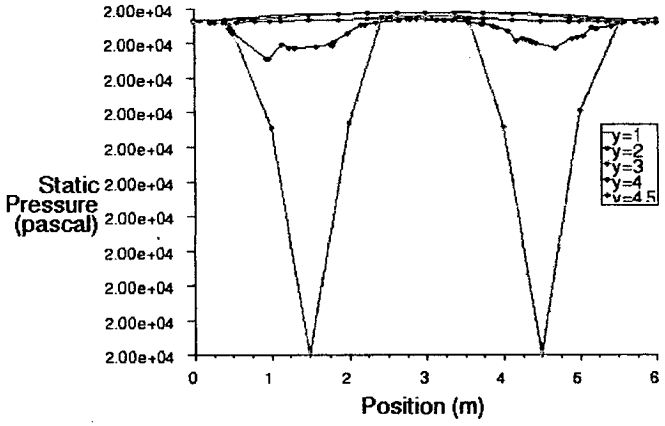

Fig 5.15 Plots of pressure at x=2 along the width of the room.

From Fig 5.15 pressure is maximum at z= 0 for all value of y. The pressure at y= 4.5 m is decreasing to minimum between z= 1 m and z= 2 m and between z=4 m and z= 5

and then increasing to maximum between z= 2 m and z=4 m. The pressure for remaining values of y is uniform along the length of the room.

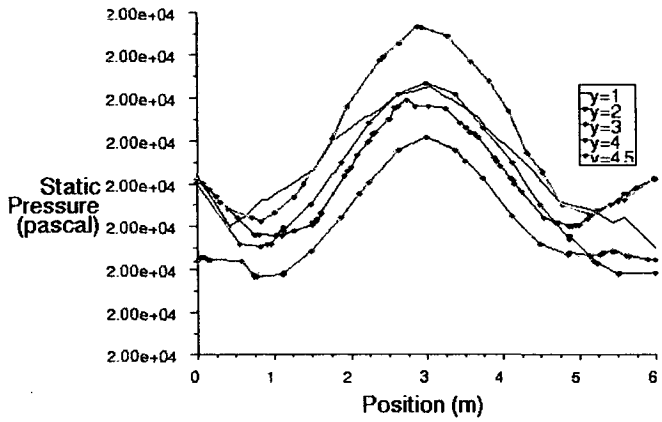

Fig 5.16 Plots of pressure at x=4 along the width of the room.

From Fig 5.16 pressure distribution is same for all values of y along the width of the room. The pressure is going to maximum between z= 2 m and z= 4 m and then decreasing gradually but the pressure at y =4 is increasing from z= 5 m to z=6 m due to the effect of windows.

5.2 RESULTS AND DISCUSSIONS OF MODEL 2

In model 2 the walls are set at different temperatures. The temperatures are as given in Table. Here also k-ε turbulence model has been used. The below results are obtained for inlet velocity of 1 m/s and sucking pressure of exhausts is 0.3 bar. The convergence criterion is as given in Table. The solution is getting converged in 395 iterations.

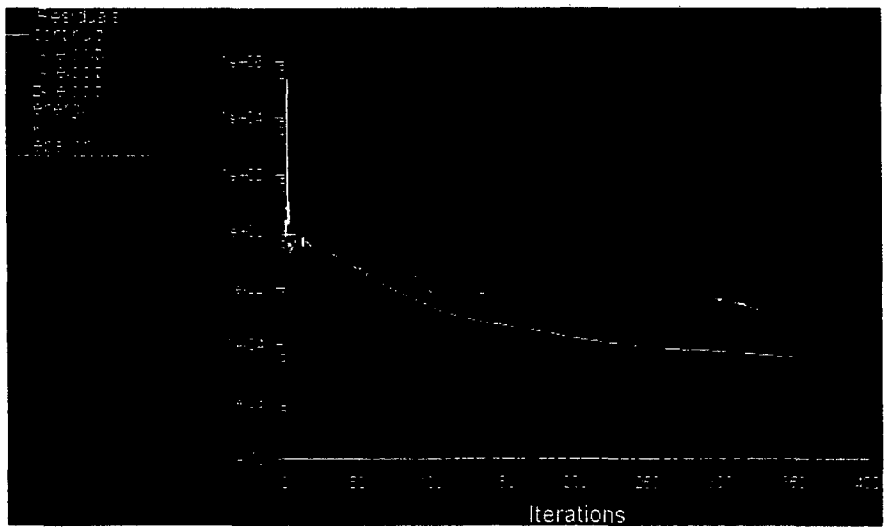

Fig 5.17 Scale residuals

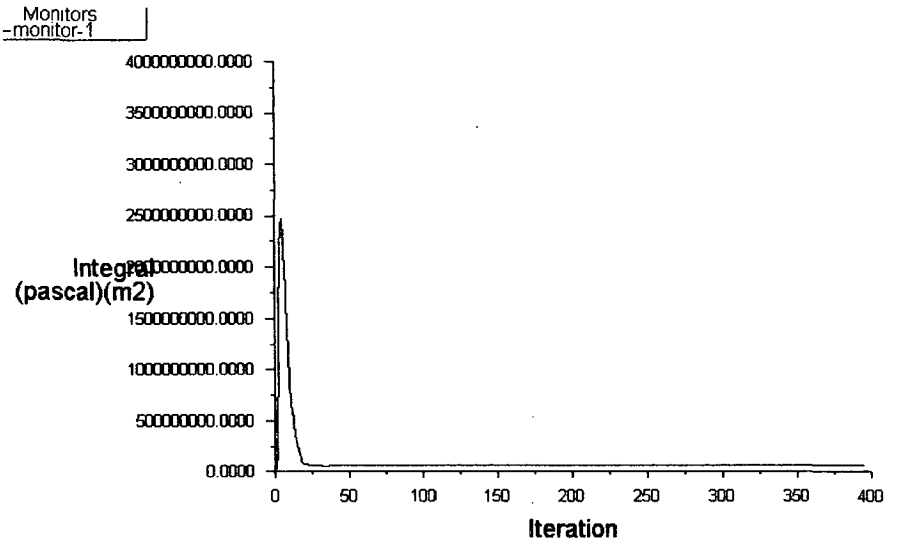

Fig 5.18 Convergence history of static pressure on interior of model 2

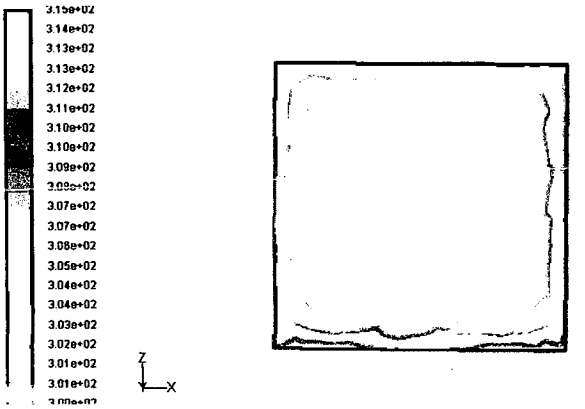

Fig 5.19 contours of temperature at y=1 m

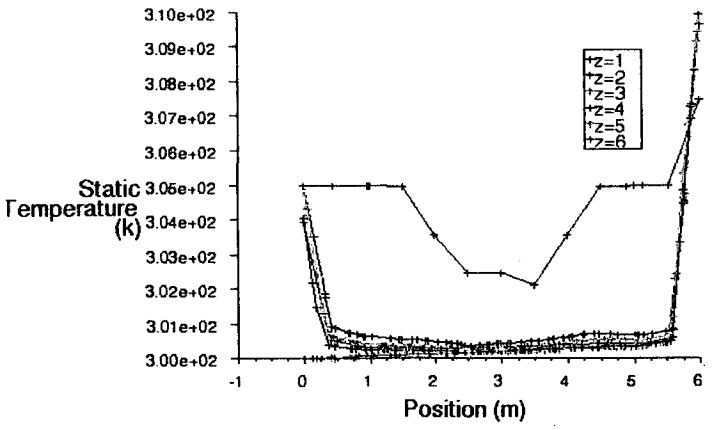

5.20 Plots of temperature at y=1 along the length of the room.

From Fig 5.19, Fig 5.20 the temperature is having high value at adjacent to the walls, temperature at x=0 m, z= 2 m is 305 K, this temperature is decreasing to around 302 K between x= 2 m and x= 4 m, then the temperature is increasing to maximum i.e. 310 K at x= 6 m. The temperature at the inlet is 300 K, and the value within the room is minimum i.e. 300 K.

The temperature distribution for remaining values of z is almost same along the room length, starting from 305 K and gradually decreasing to 300 K and then increasing to 310 K at x=6 m.

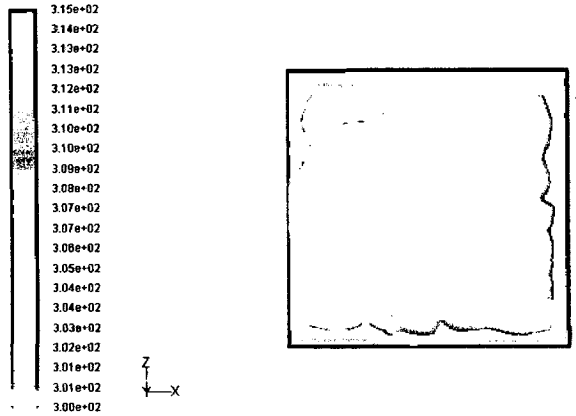

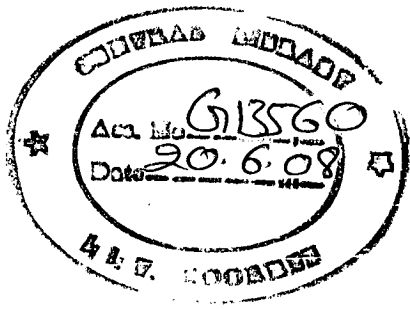

Fig 5.21 contours of temperature at y=2 m

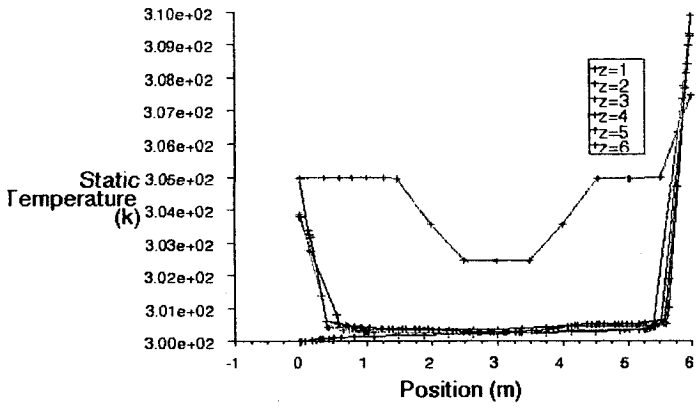

5. 22 Plots of temperature at y=2 along the length of the room

From Fig 5.21, Fig 5.22 the temperature distribution is almost same as at height of y=1 m. the temperature at the inlet is 300 K. The average temperature within the room is 300 K. The temperature is high at adjacent to the walls i.e. 305 K to 315 K

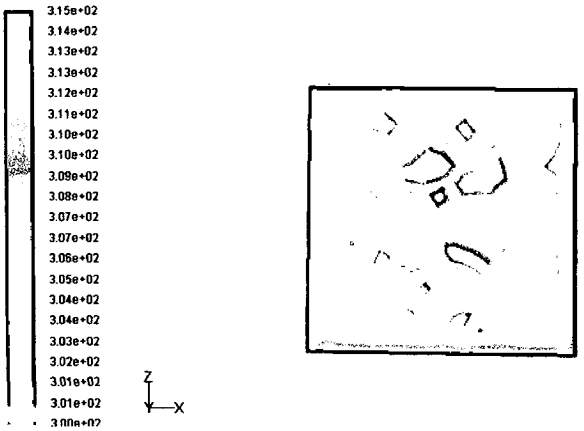

Fig 5.23 contours of temperature at y=4 m

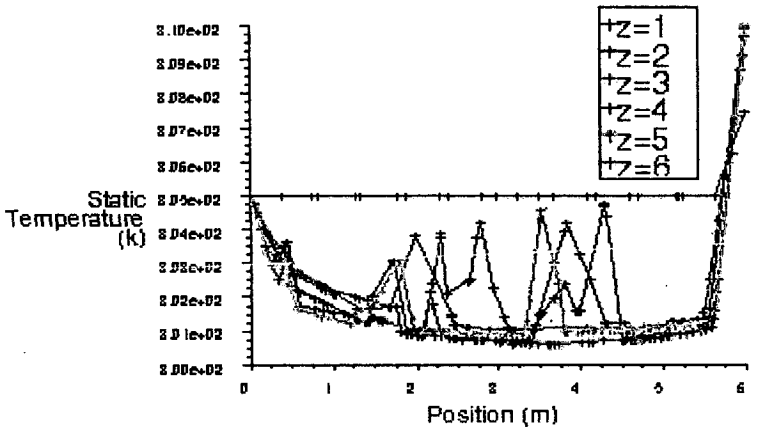

5.24 Plots of temperature at y=4 along the length of the room

From Fig 5.23, Fig 5.24 the temperature within the room is fluctuating between 301 K and 305 K. The temperature is higher at adjacent to the walls. The temperature at height of y= 4 m and at x= 0 m, z=6 is 305 K and this temperature is uniform till x=5.5 m, then increasing to 308 K. The temperature of z=3 m surface is starting from 305 K at x= 0 m and then gradually decreasing along the length of the room and is 301 K at x=6 m. The temperature for z=1 m, z= 2 m,z= 4 m and z=5 m surfaces is fluctuating between 301 k to 305 K.

In model 2 the walls are set at different temperatures. The temperature distribution at height of y= 1m and height of y= 2 m is almost same. At both of these heights the temperature at inlet is 300 K; this is the temperature of entering air. The average temperature within the room is 300 K. The temperature is high at adjacent to the walls i.e. 305 K to 315 K.

The temperature distribution at height of y= 4 m is not effected by the inlet and windows. Temperature within the room is fluctuating between 301 K and 305 K at this height. In the middle of the room at around x= 3 m, temperature is 300k. The effect of temperature of walls into the room is higher at this height than at height y=1 m and y= 2m.

RECOMMENDATIONS FOR FUTURE WORK

In this dissertation the velocity -, pressure - and temperature - profiles are studied at steady state. In this work two different models are considered. In future, the work can be extended to the study of temperature profiles with the heat generation within the room and heat flux though walls.

Unsteady states can be studied for sudden emission of pollutants or contaminants and/or energy release. In this project the simulation is carried out using only one CFD package namely, Fluent software, for comparison simulation runs can also be carried out using other CFD packages like Phoenics and CFX etc.

In this study only k-ε turbulence model have been used to study flow , it can be extended to include other turbulence models for comparison and better understanding of air flow inside a room.

1. Awbi, H.B., "Application of Computational Fluid Dynamics in Room Ventilation." Journal of Building and Environment. Vol. 24, No. 1. (1989).
2. Baker, A.J. and Kelso, R.M., "On Validation of Computational Fluid Dynamics Procedures for Room Air Motion Prediction." ASHRAE Transactions,Vol. 96, No. 1(1990).
3. Chen, Q., Moser, A. and Huber, A., "Prediction of Buoyant, Turbulent Flow by a low-Reynolds Number k-ε Model." ASHRAE Transactions, Vol.96, Pt.1. (1990).
4. Espi, E., Berne, Ph. and P.Duverneuil,"Using CFD to understand the air circulation in a ventilated room", journal of computers chem. Engineering Vol.22, supl.p.751-754. (1998)
5. Ferziger, J.H., Peric, M., "Computational Methods for Fluid Dynamics", 3rd edition, Springer Publishing, (2002).
6. Hinze, J.O. Turbulence (2nd Edition). McGraw-Hill. New York. (1987)
7. Lam, C.G. and K. Bremhorst. "A Modified Form of the k-ε Model for Predicting Wall Turbulence." ASME Transactions. Vol. 103. (1981)
8. Launder, B.E ,and Spalding, D.B., " The numerical computation of Turbulent flow", Journal of Computer Methods in Applied Mechanics and Engineering, Vol.3,p.269-289. (1974).
9. Launder, B. E., & Spalding, D. B. Mathematical models of turbulence. London, England: Academic Press Inc Ltd. (1972).
10. Murakami, S. and Kato, S., "Numerical and Experimental Study on Room Airflow 3- D Predictions using the k-e Turbulence Model", Journal of Building and Environment, Vol. 24, 1989, No.1. p.85-97.
11. Murakami, S. and Mochida, A. "Three-Dimensional Numerical Simulation of Turbulent Flow Around Buildings using the k-ε Turbulence Model", Journal of Building and Environment. Vol 24, No. 1. P.51-54. (1989)
12. Murakami, S. and Suyama, Y., "Numerical and Experimental study on Turbulence Diffusion fields in conventional flow type clean rooms", ASHRAE Transactions Vol.94, Pt.2 (1988).

13. Murakami, S., Kato, S. and Suyama, Y., "Three-Dimensional numerical simulation of Turbulent airflow in a ventilated room by means of a two-equations model", ASHRAE Transactions,Vol.93,Pt.2(1987).

14. Patel,V.C., W. Rodi, and G. Scheurer. "Turbulent Models for Near-Wall and low-Reynolds Number Flows: A Review." AIAA Journal. Vol. 23, No. 9. (1984)

15. Peter V. Nielson, "The selection of Turbulence Models for Prediction of Room Airflow", ASHRAE Transactions, Vol.10, p.1119-1127. (1998)

16. Pitarma, R.A., Ramos, J.E., Ferreira, M.E. and Carvalho, M.G., "Computational Fluid Dynamics: An advanced active tool in environmental management and education", Management of Environmental Quality: An International Journal Vol. 15 No. 2, pp. 102-110,(2004).

17.Reinartz, A. and Renz, U., "Calculation of the temperature and flow field in a room ventilated by a radial air distributor", International Journal of Refrigeration, Vol.7, No.5, p.308-312. (1984)

18.Rodi, W. "Turbulence Models for Environmental Problems." Prediction Methods for Turbulent Flows. W. Kollman, ed. Hemisphere/McGraw-Hill. New York. (1980)

19. Spitler, J.D. "An Experimental Investigation of Air Flow and Convective Heat Transfer in Enclosures Having Large Ventilative Rates." Ph.D. Thesis. Department of Mechanical and Industrial Engineering, University of Illinois at Urbana-Champaign. (1990)

20 Spitler, J.D.,C.O. Pederson, D.E. Fisher, P.F. Menne, and J. Cantillo. "An Experimental Facility for Investigation of Interior Convective Heat Transfer." ASHRAE Transactions. Vol. 97, Pt. 1. (1991)

21 WREC 1996,"Air Movement in Naturally-Ventilated Buildings", p. 241- 246.

22. Zhang Lin, Chow, T.T., Tsang, C.F., Fong, K.F. and Chan, L.S., "CFD study on effect of the air supply location on the performance of the displacement ventilation system", Journal of Building and Environment 40,p. 1051-1067. (2005).